超 冷 的 水

牟中原
台灣大學化學系
cymou@ntu.edu.tw

生物圈

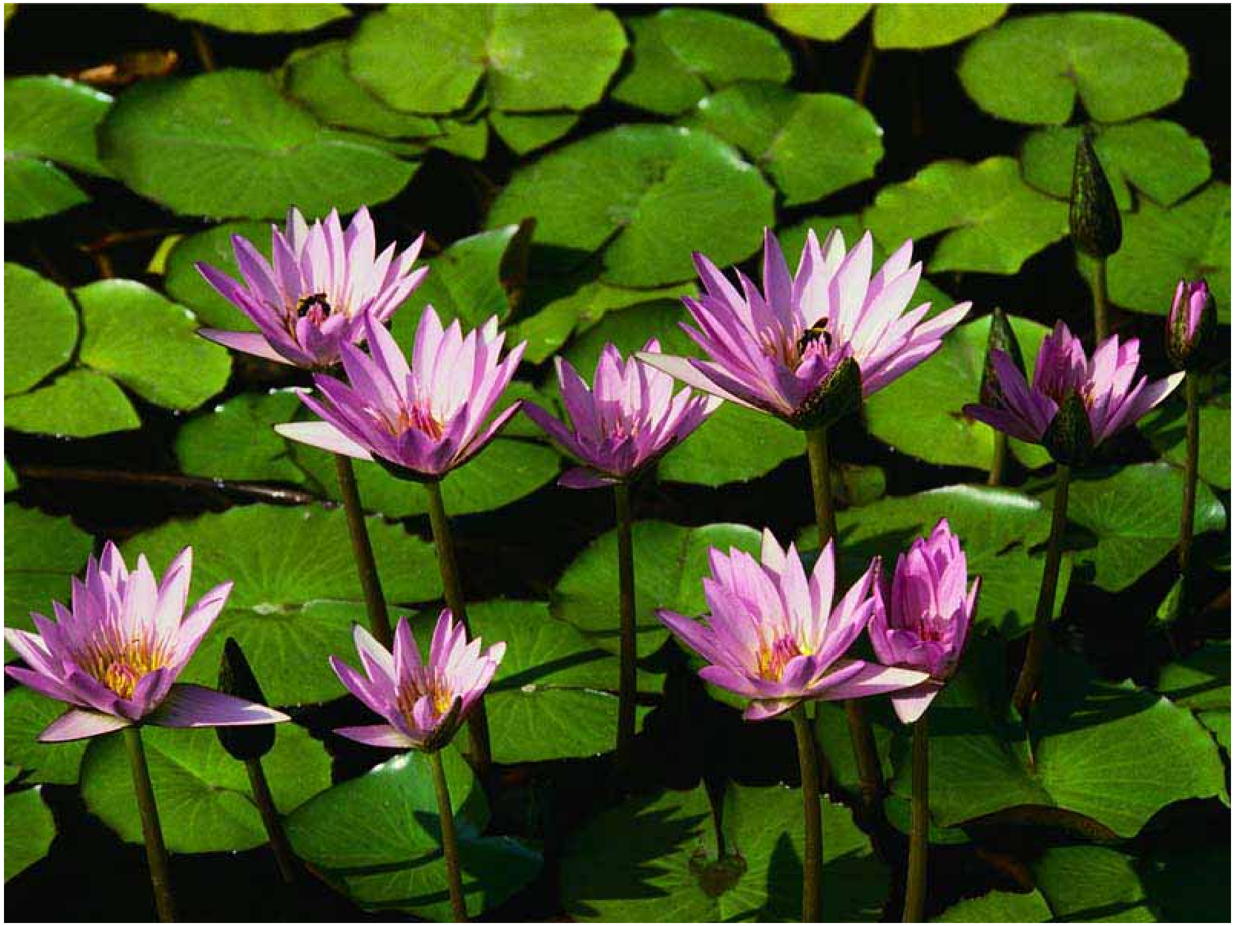

ABNORMAL PROPERTIES OF WATER

- Negative volume of melting(**12% on melting)**
- Density maximum at 4°C
- Isothermal compressibility (K) minimum at 46 °C
- Minimum heat capacity Cp at 35 °C
- has the highest heat of vaporization per gram of any liquid.
- Anomalously high mp and bp
- Many crystalline forms (11 at least)
- Increasing fluidity with increasing pressure
- Cp and K diverge at -46 °C
- Hydrophobic effect

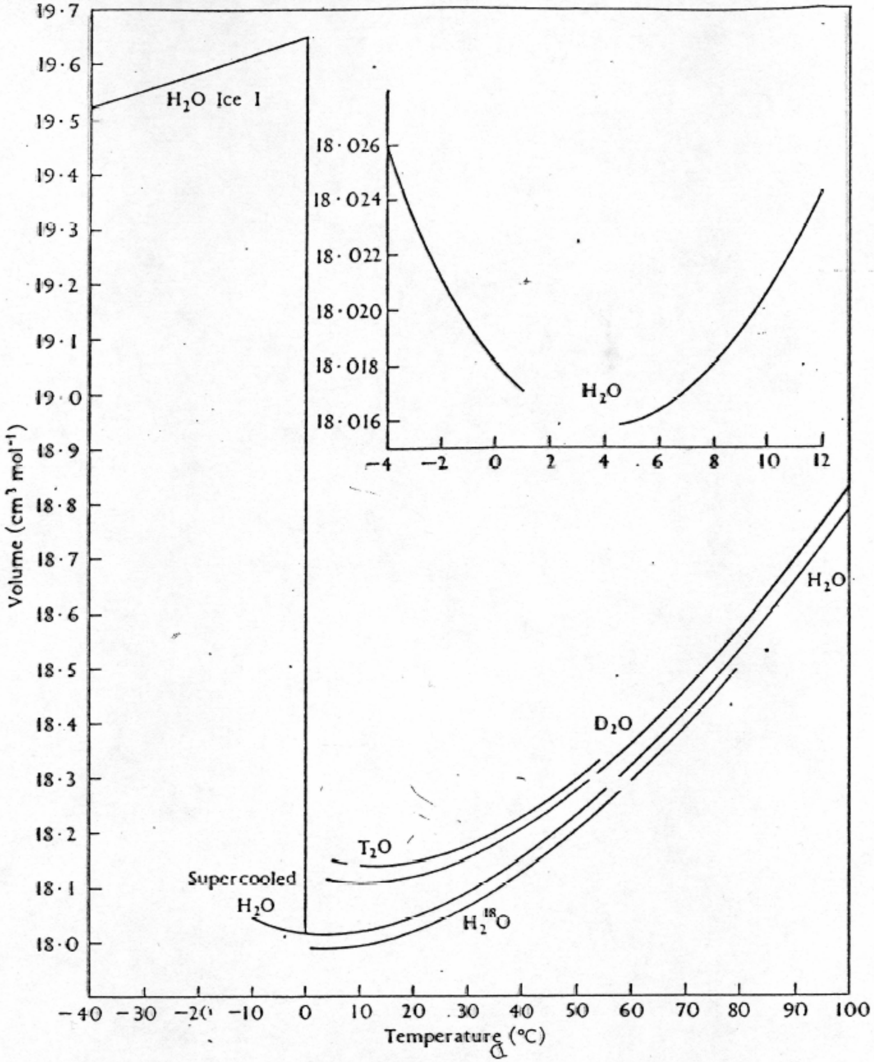

FIG. 4.13. The molar volumes of H_2O ice I and four isotopic liquid waters at 1 atm pressure. The inset is an enlargement of the curve for liquid H_2O between −4 and +12 °C. The data for ice I are from Table 3.10 (*b*). The curves for the liquid were calculated from eqn (4.6) and the following molecular weights: H_2O, 18·0153; D_2O, 20·028; $H_2{}^{18}O$, 20·015; T_2O, 22·04.

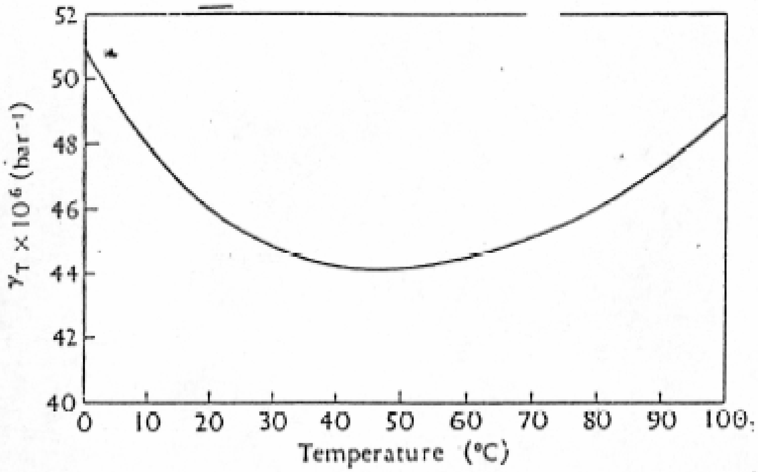

FIG. 4.15. The coefficient of isothermal compressibility, γ_T, for liquid water at 1 atm pressure. Data from Kell (1967).

What is the puzzle of liquid water?

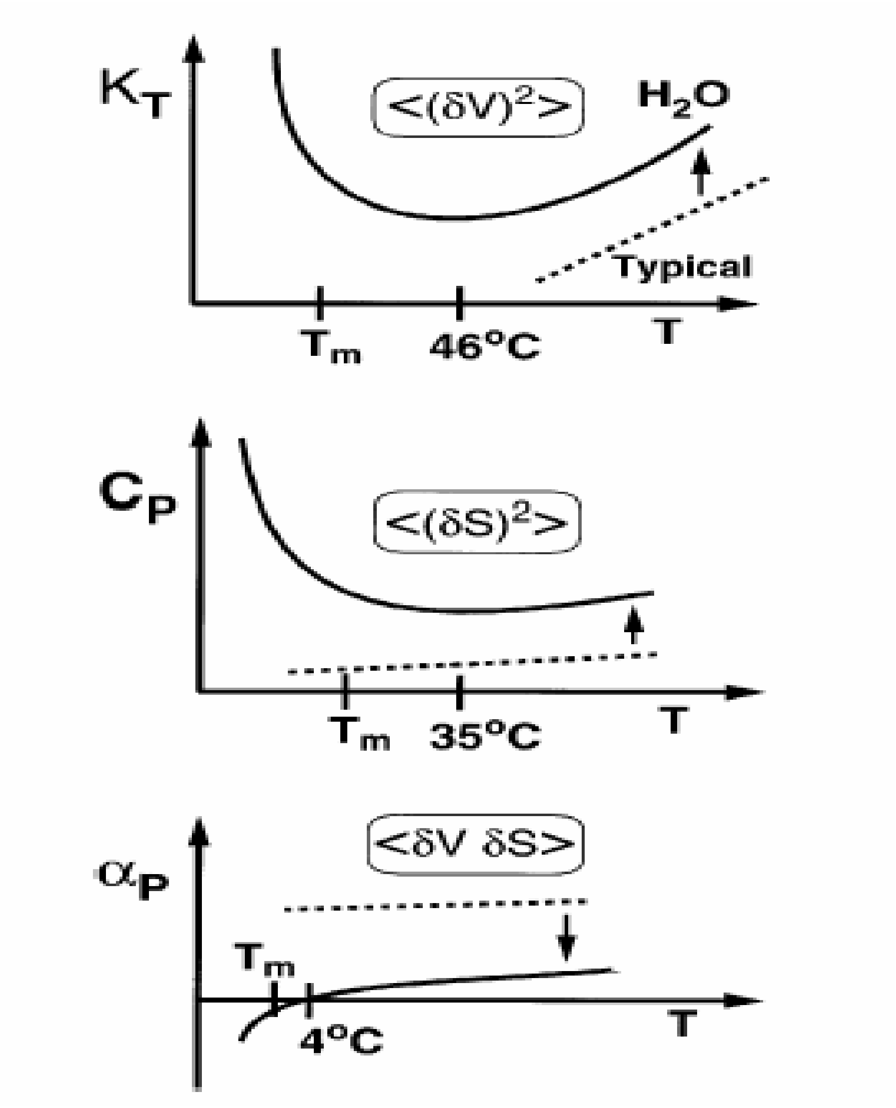

Minimum
Compressibility at 46 ^{o}C

Minimum heat capacity
at 35 ^{o}C

Maximum Density at 4 ^{o}C

一純物質

可不可能有兩個液相共存？

PHASE RULE

$$F = C - P + 2$$

- **The laws of thermodynamics permit the liquid region of the phase diagram for a pure substance to be subdivided into distinct phases**
- **Then, why are L-L transition not commonly observed?**

1. **exploration of a wide range of P and T may be required (order parameter= ρ)**
2. **most likely to be metastable transitions observed in the supercooled liquid state(nucleation of solid)**
3. **A L-L transition in a supercooled liquid may also be obscured by the glass transition.**

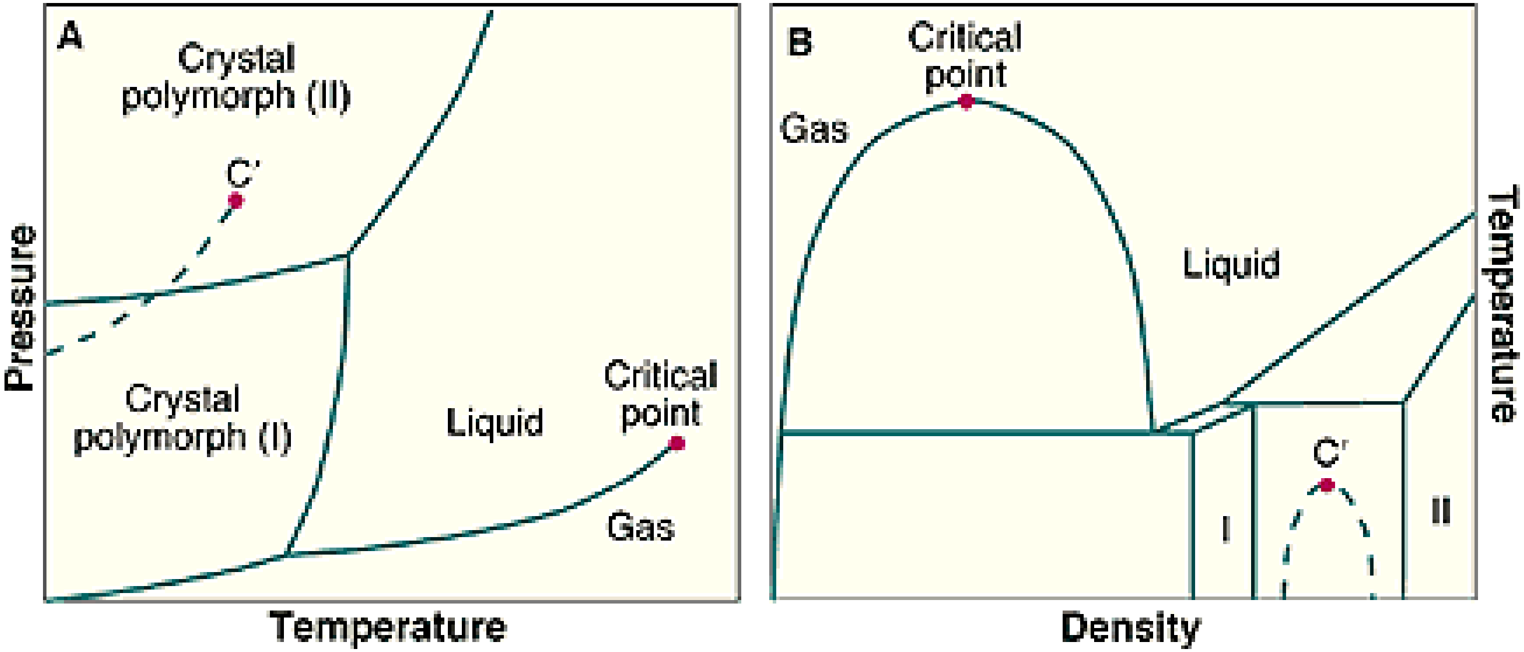

Schematic phase diagram: The liquid-gas coexistence line terminates in the critical point. The dashed line is the coexistence line for a liquid-liquid phase transition in the supercooled liquid, terminating in a critical point C′. (**B**) Projection of the lines given in (A) into the plane of temperature and density.

Likely candidates

Liquids having open molecular coordination environments at low pressure. Notably, these include liquids with a locally tetrahedral molecular structure, such as

Si, Ge, C, SiO_2, GeO_2, and H_2O itself

Kurita and Tanaka, Science, 306, 845 (2004)

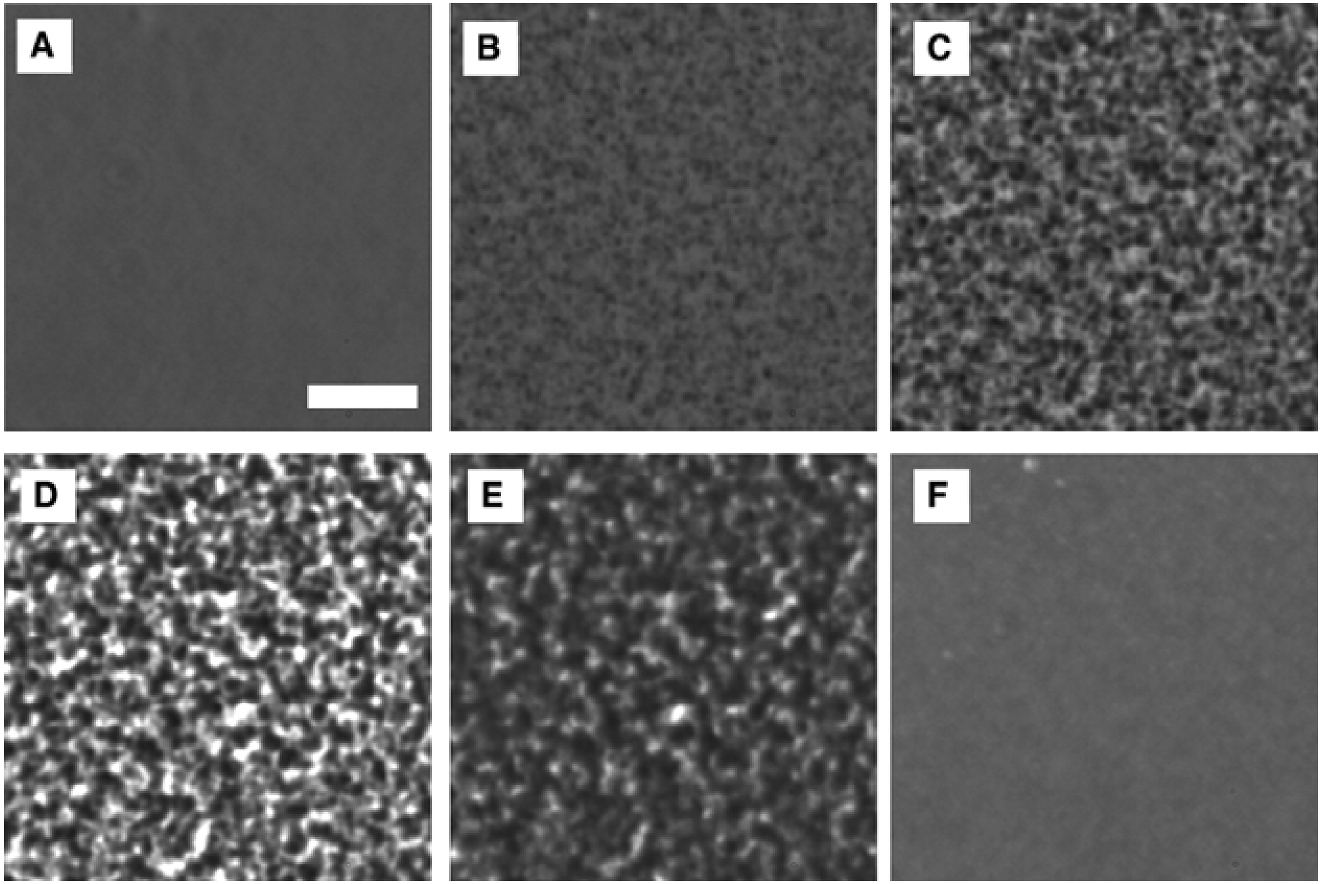

$:P(C_6H_5)_3$

Pattern evolution process during the transformation of liquid I to liquid II, observed with phase contrast microscopy at 212 K. Time *t* was 75 min (**A**), 90 min (**B**), 120 min (**C**), 150 min (**D**), 210 min (**E**), and 400 min (**F**) after the temperature quench.

Thermodynamic Properties of Supercooled Water

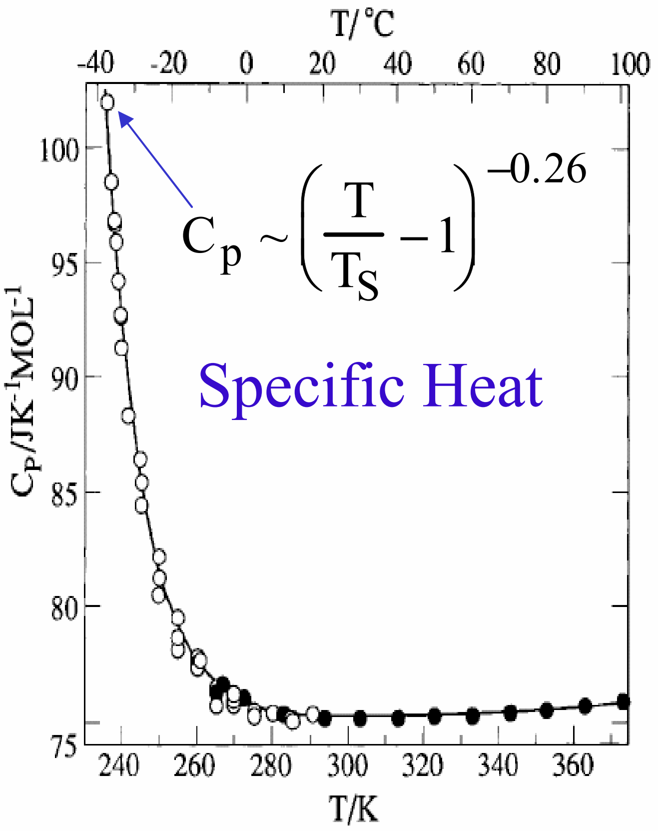

$$C_p \sim \left(\frac{T}{T_S} - 1\right)^{-0.26}$$

Specific Heat

Figure 11. The temperature dependence of supercooled water's isobaric heat capacity c_p at atmospheric pressure. Literature data (●) included in the original [69], as well as measurements of Angell *et al* (○). Reprinted, with permission, from [24], Debenedetti P G, *Metastable Liquids, Concepts and Principles* copyright (1996) Princeton University Press, and adapted originally from [69].

$$T_S = 228\ \text{K}$$

$$= -45\ ^{\circ}\text{C}$$

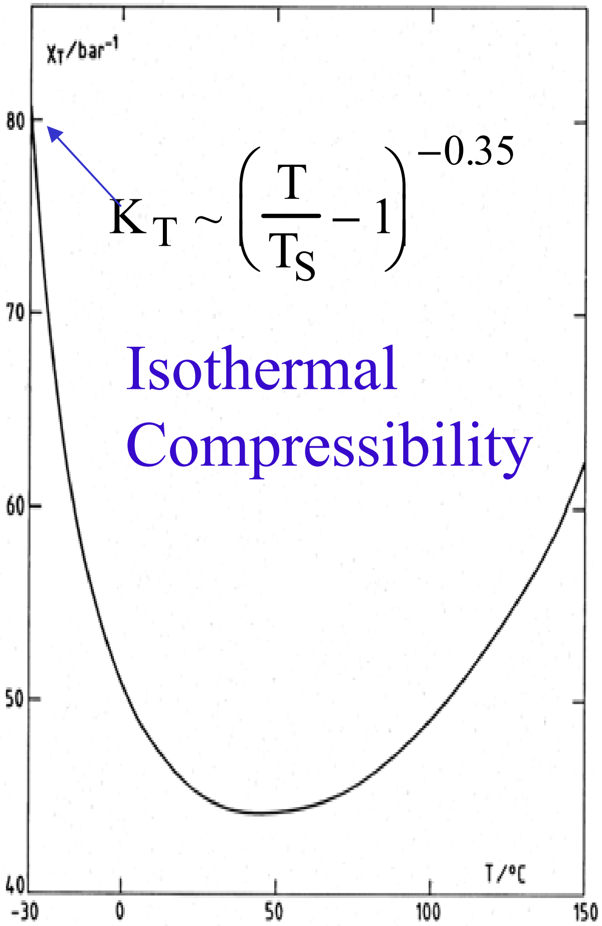

$$K_T \sim \left(\frac{T}{T_S} - 1\right)^{-0.35}$$

Isothermal Compressibility

Figure 2. Isothermal compressibility of H_2O as a function of temperature. Taken from G. S. Kell, *J. Chem. Eng. Data* **20,** 97 (1975).

C. A. Angell, et al, *JPC* **77**, 3092 (1973)

R. J. Speedy, et al, *JCP* **65**, 851 (1976)

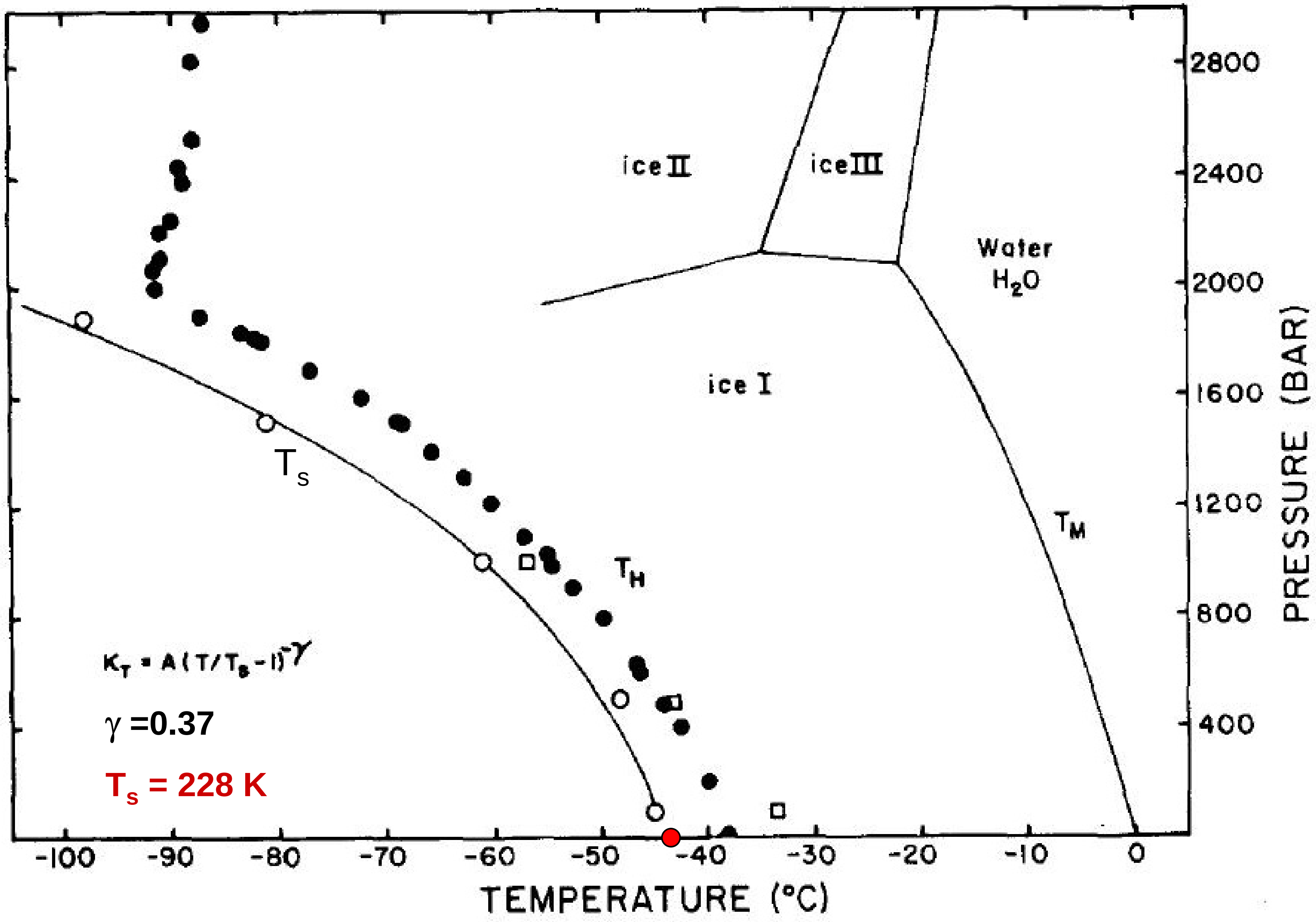

H. Kanno, and C. A. Angell, JCP, **70**, 4008, 1978

Walrafen, Hokmabadi, and Yang: Isosbestic points from water

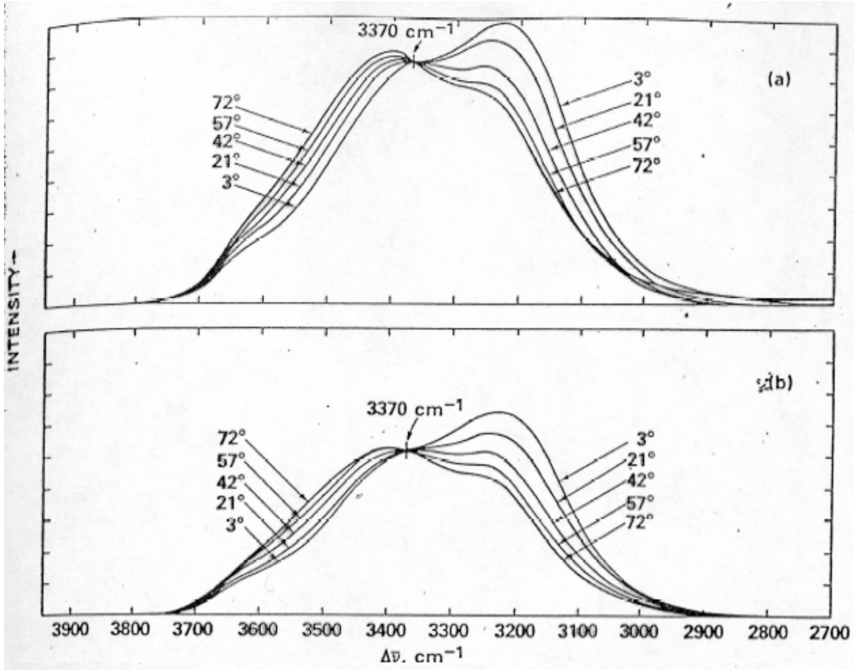

FIG. 3. Isotropic Raman spectra from water between 3 and 72 °C. (a) refers to $X(ZZ)Y-(4/3)X(ZX)Y=45\alpha^2$, and (b) refers to: $X(Z,X+Z)Y-(7/6)X(Y,X+Z)Y=45\alpha^2$. (a) intensities are increased relative to the (b) intensities, e.g., the scaling factor is evident at 3370 cm^{-1}, the isosbestic point.

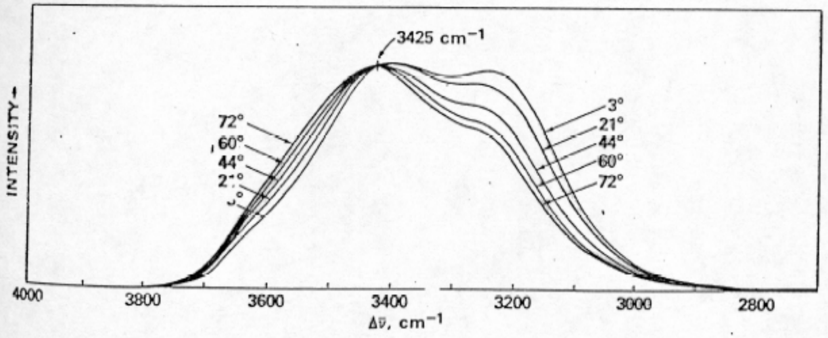

FIG. 4. Absolute Raman spectra in the OH-stretching region from water between 3 and 72 °C for the orientation $X(Z,X+Z)Y$. $X+Z$ means that both the X and Z polarizations of the Raman scattering were collected. Isosbestic point, 3425 cm^{-1}.

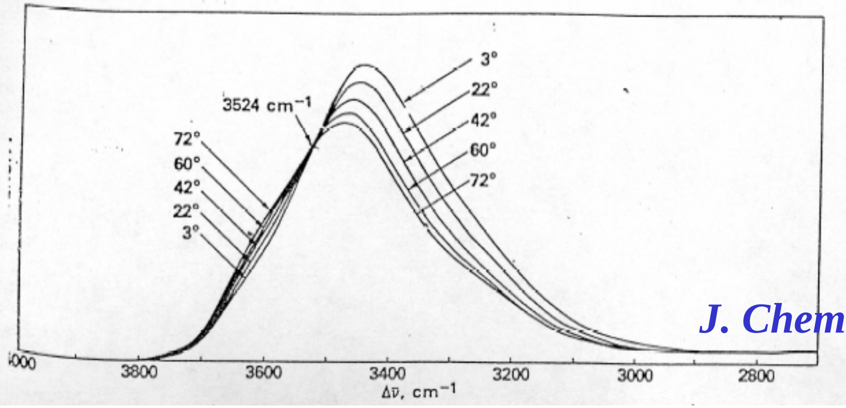

FIG. 5. Absolute Raman spectra in the OH-stretching region from water between 3 and 72 °C for the orientation $X(Y,X+Z)Y$. All intensities are increased by a factor of ~3.6 relative to Fig. 4. Isosbestic point, 3524 cm^{-1}.

J. Chem. Phys. **Vol. 85, No. 12, 15 December 1986**

Hydrogen Bonding Structure

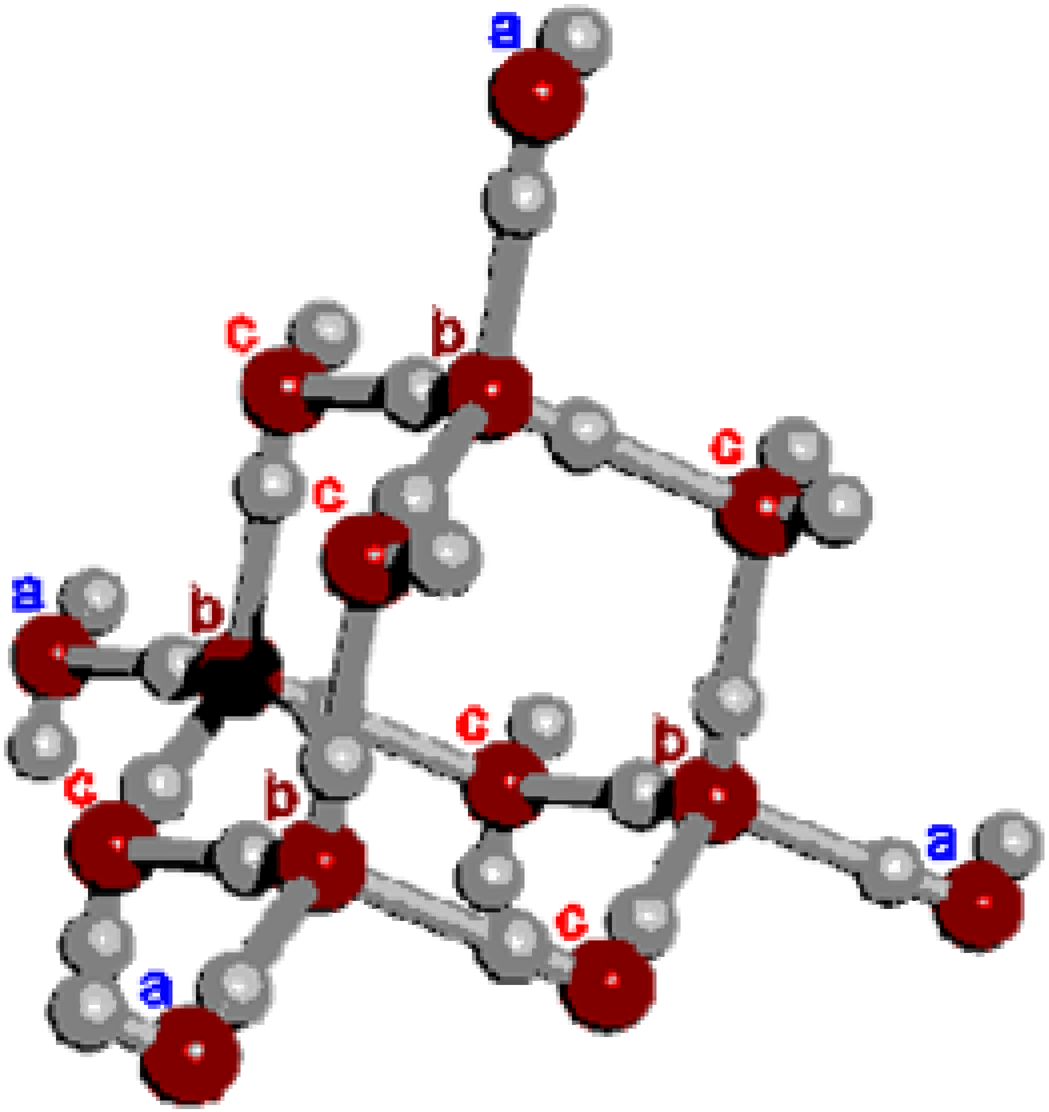

Ice –Ih

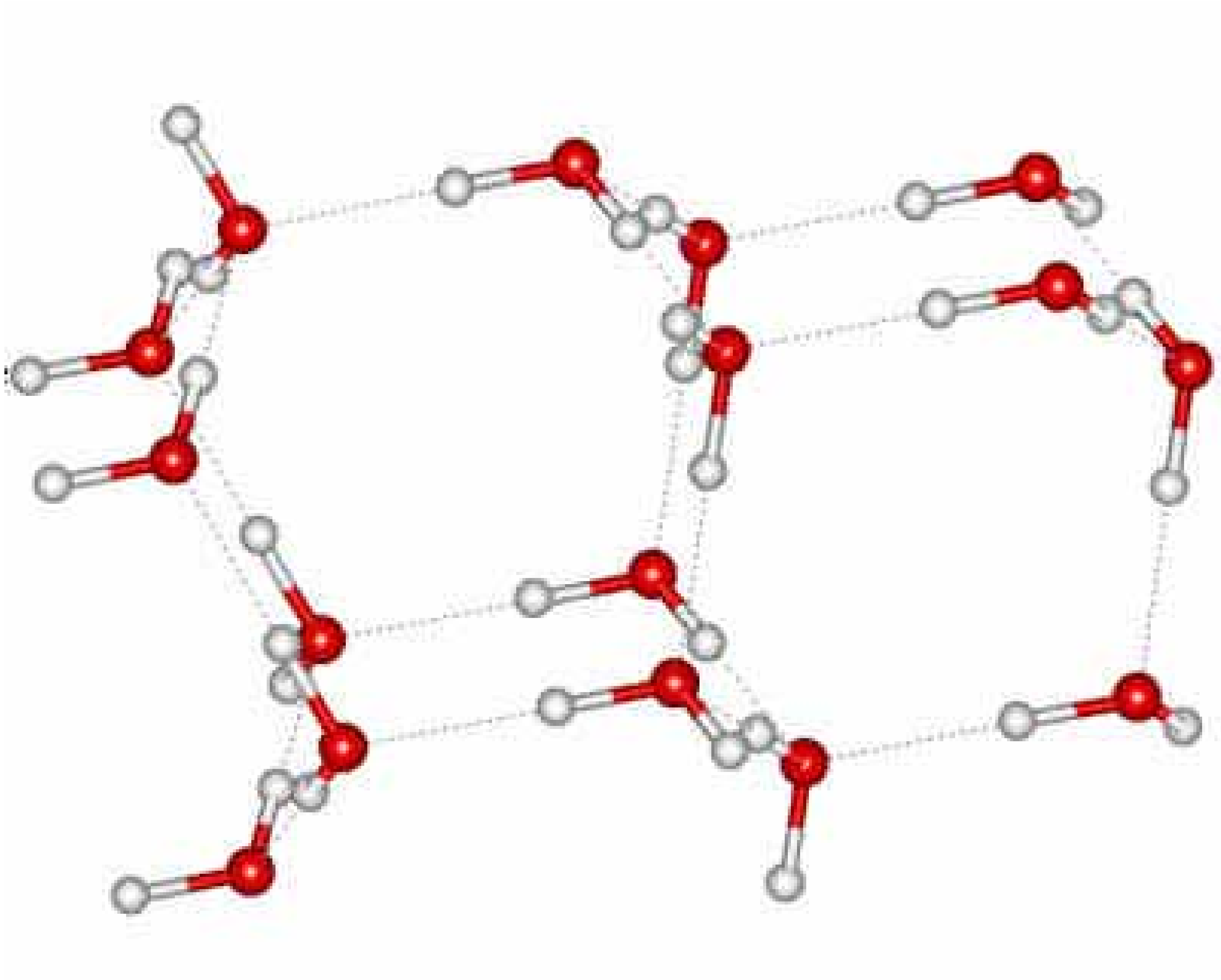

Ice VII 1.65 g cm^{-3} (at 2.5 GPa and 25°C)

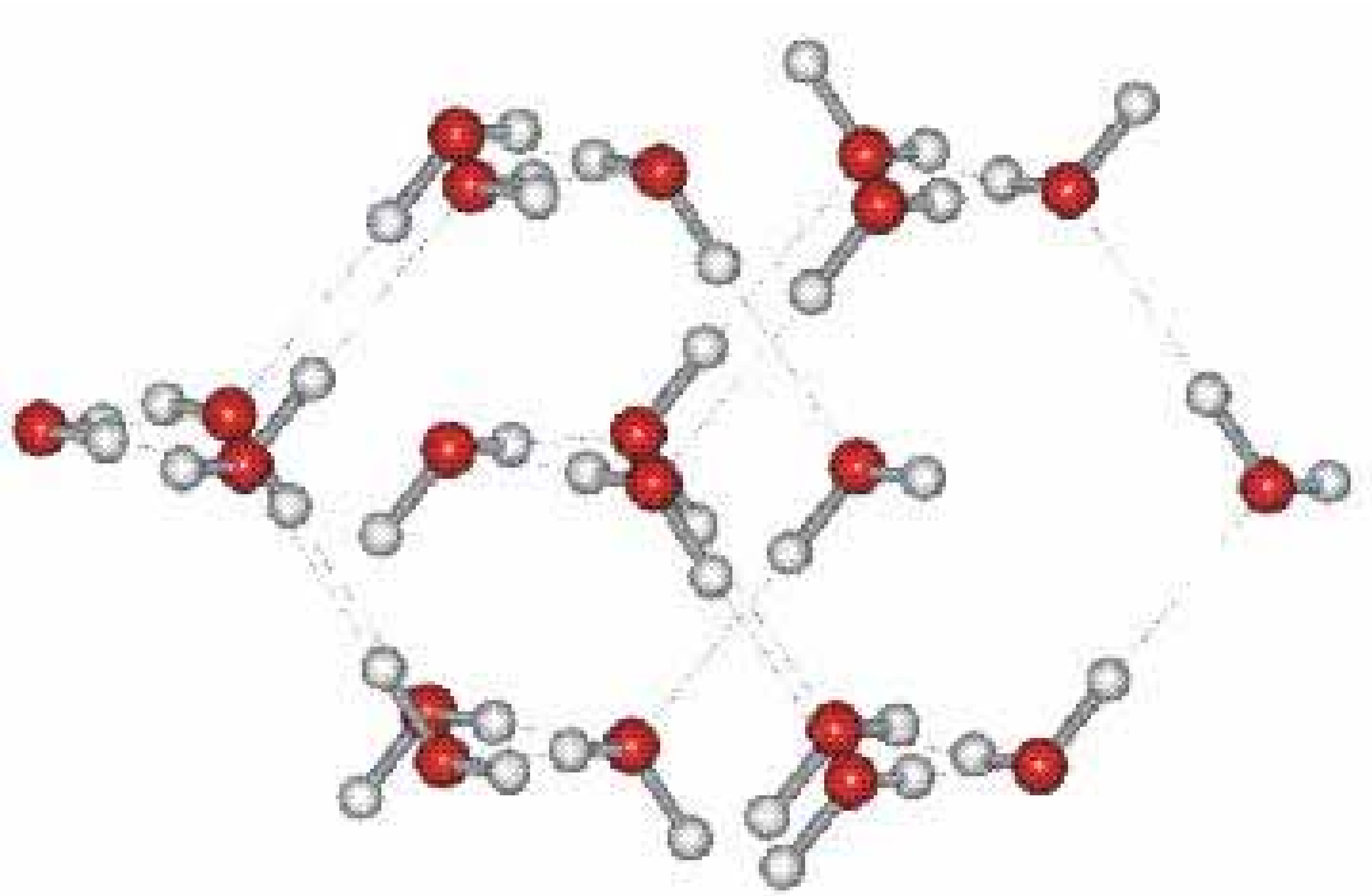

The phase diagram of water is complex

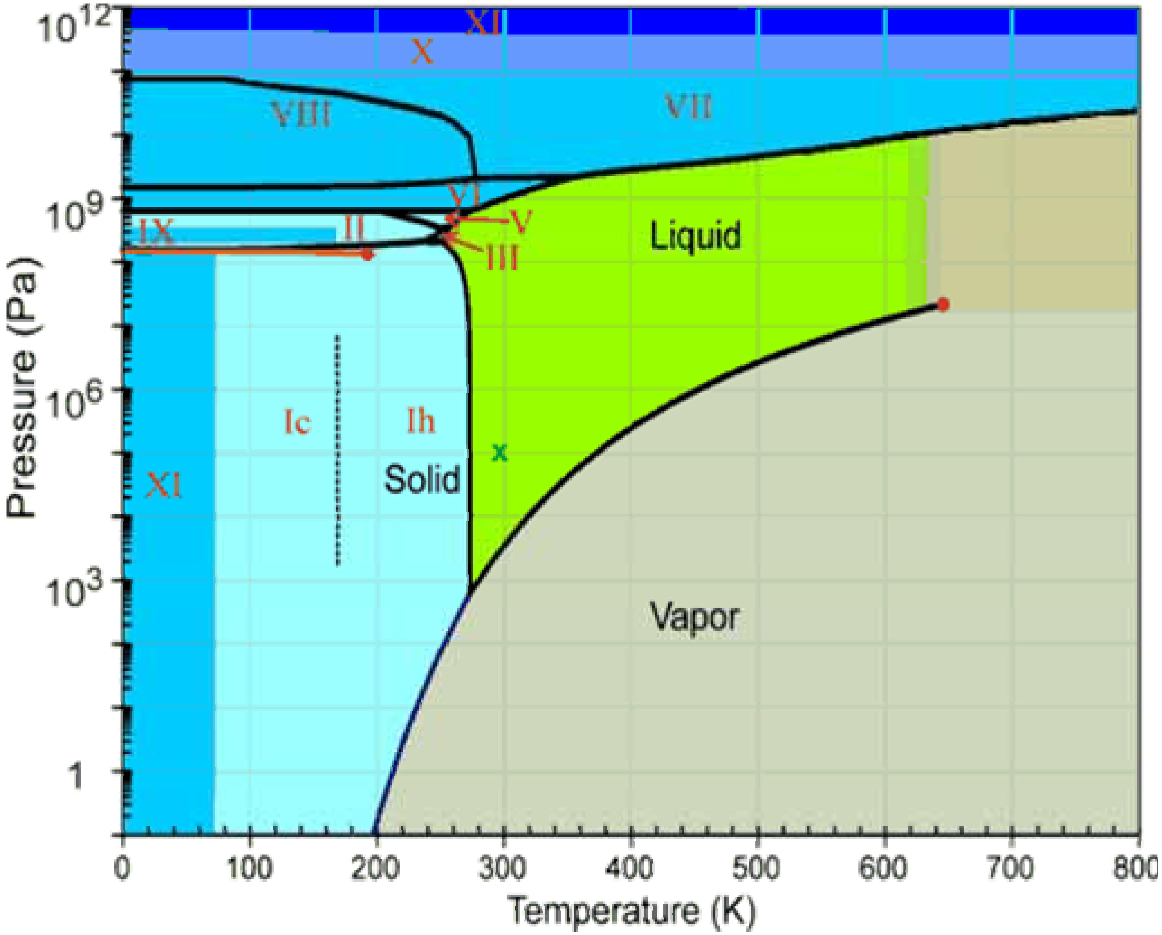

If water behaved more typically as a low molecular weight material, its phase diagram may have looked rather like this:

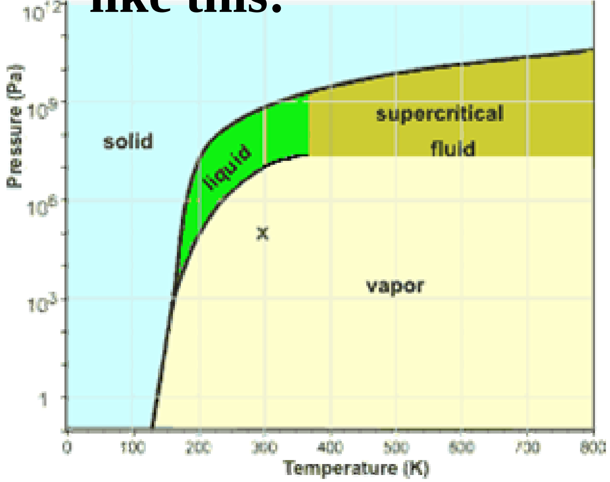

Molecular Dynamics Simulation

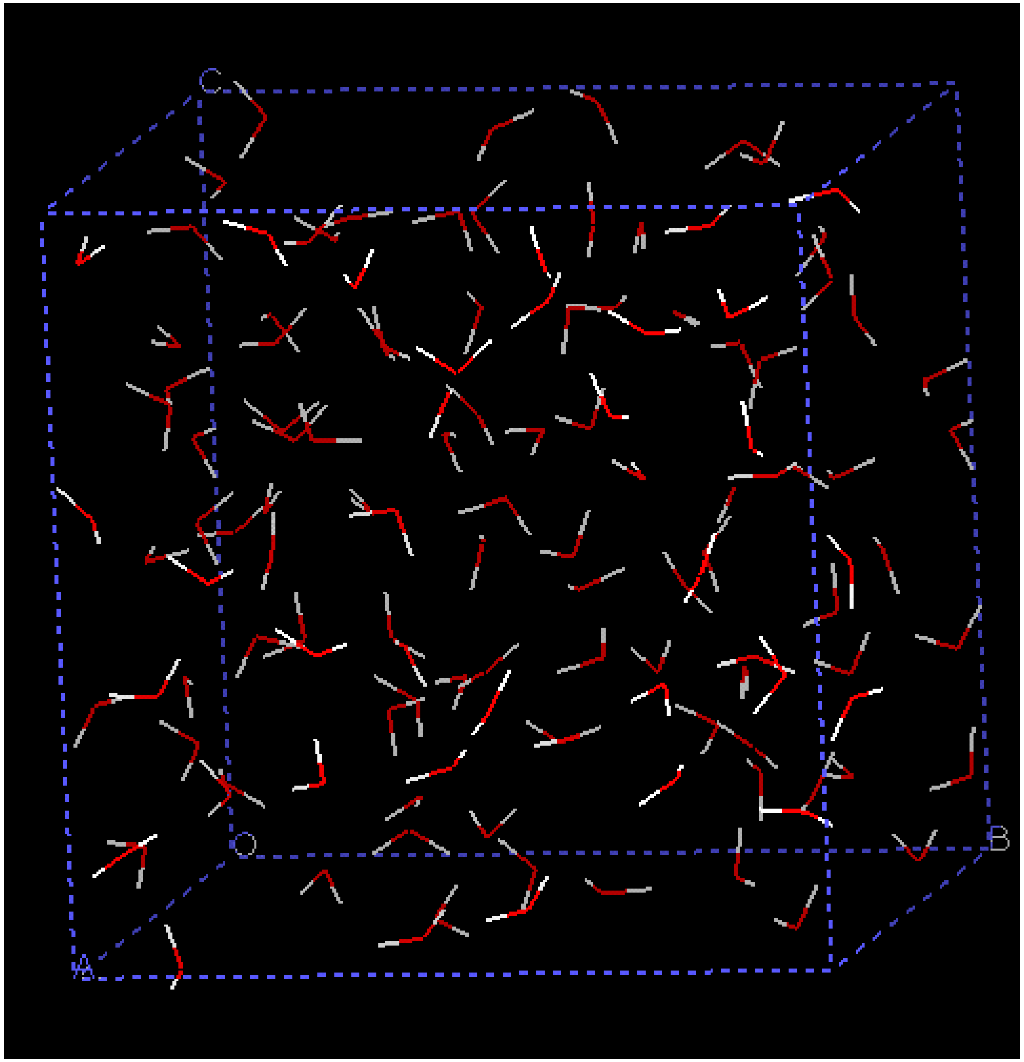

TIP4P Model

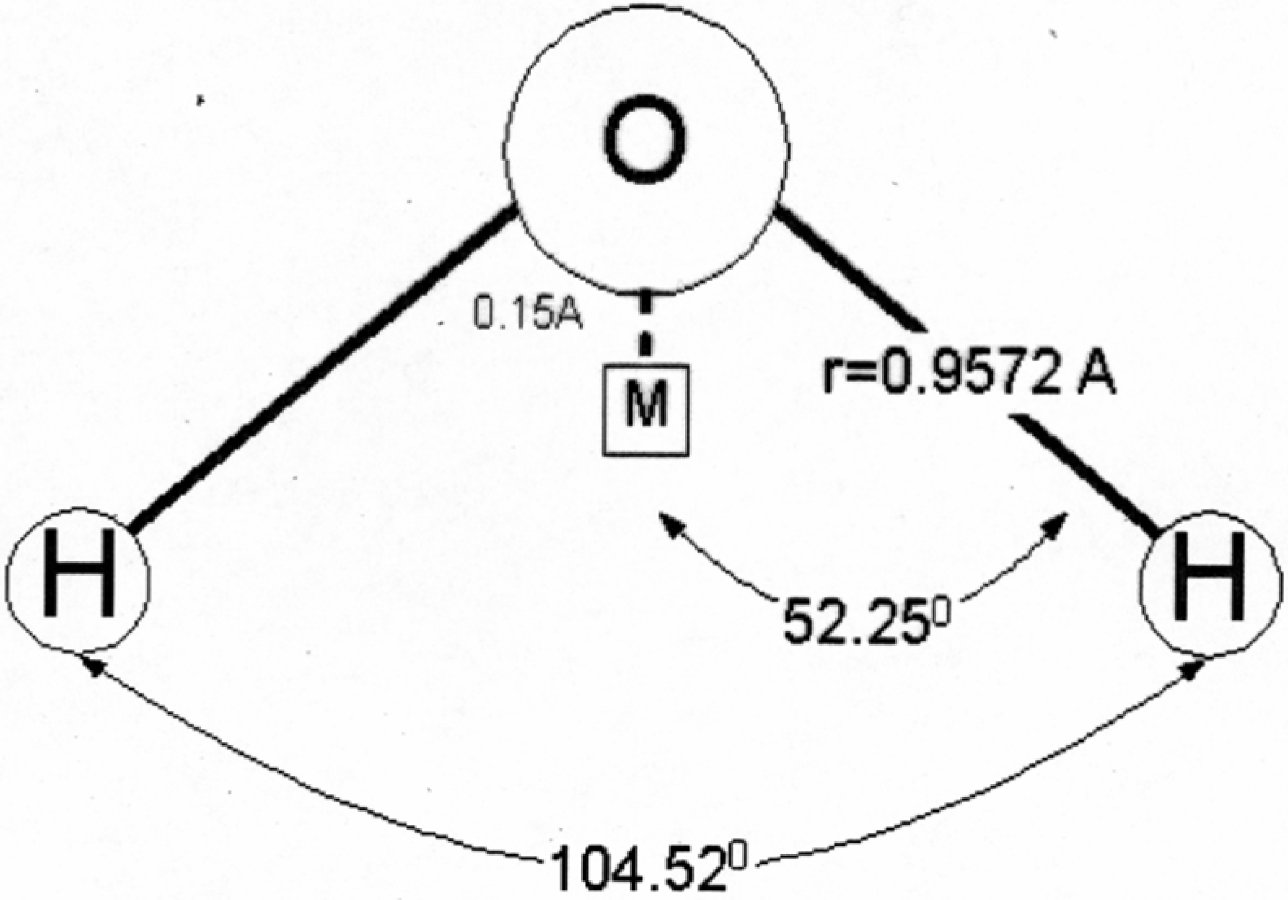

2-D Voronoi Cell

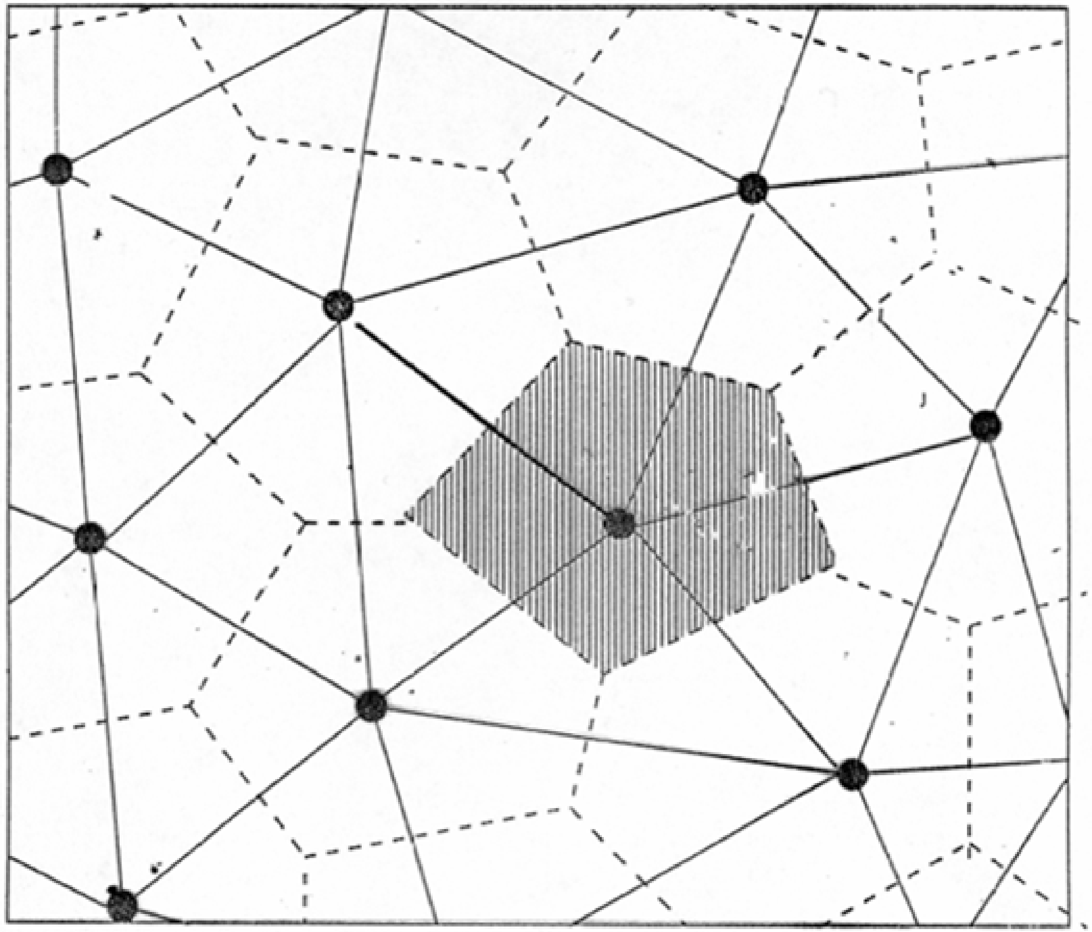

The Heavy dots denote the atomic sites, the voronoi cells are shown by the light lines, and the heady lines denote the bonds of the simplicial graph.

Voronoi Analysis

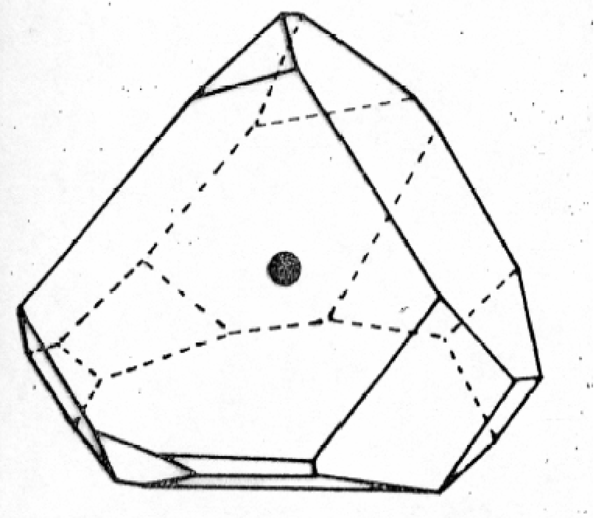

FIG. 1. Typical VP surrounding a water molecule (●) at $T \approx 250$ K.

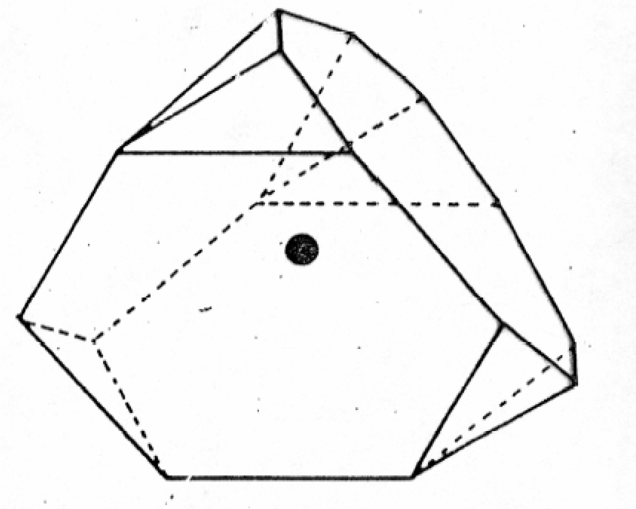

FIG. 2. The same as in Fig. 1 but for the structure of ice I_h. The point of view of the polyhedra has been chosen in order to show the similarity with the water VP in Fig. 1.

$N_f = ½ \bullet N \nu + 2$

$N_e = 3/2 \bullet N \nu$

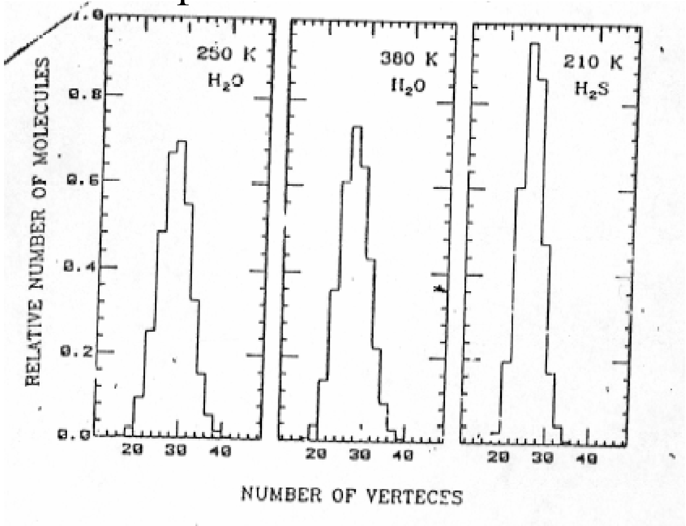

FIG. 3. Distribution of the number of vertices in H_2O at $T \approx 250$ and $T \approx 380$ K, and in H_2S at $T \approx 210$ K. Since the number of vertices is always even the histogram step is two.

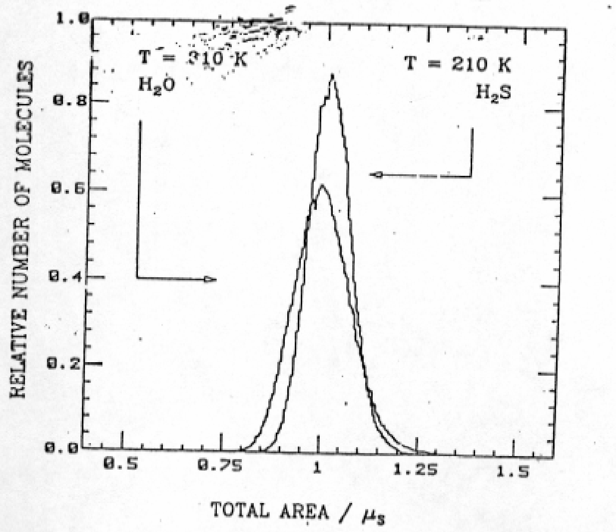

FIG. 5. Comparison of the total surface area distribution in H_2O ($T \approx 310$ K) and H_2S ($T \approx 210$ K) reported as a function of S/μ_S.

Asphericity

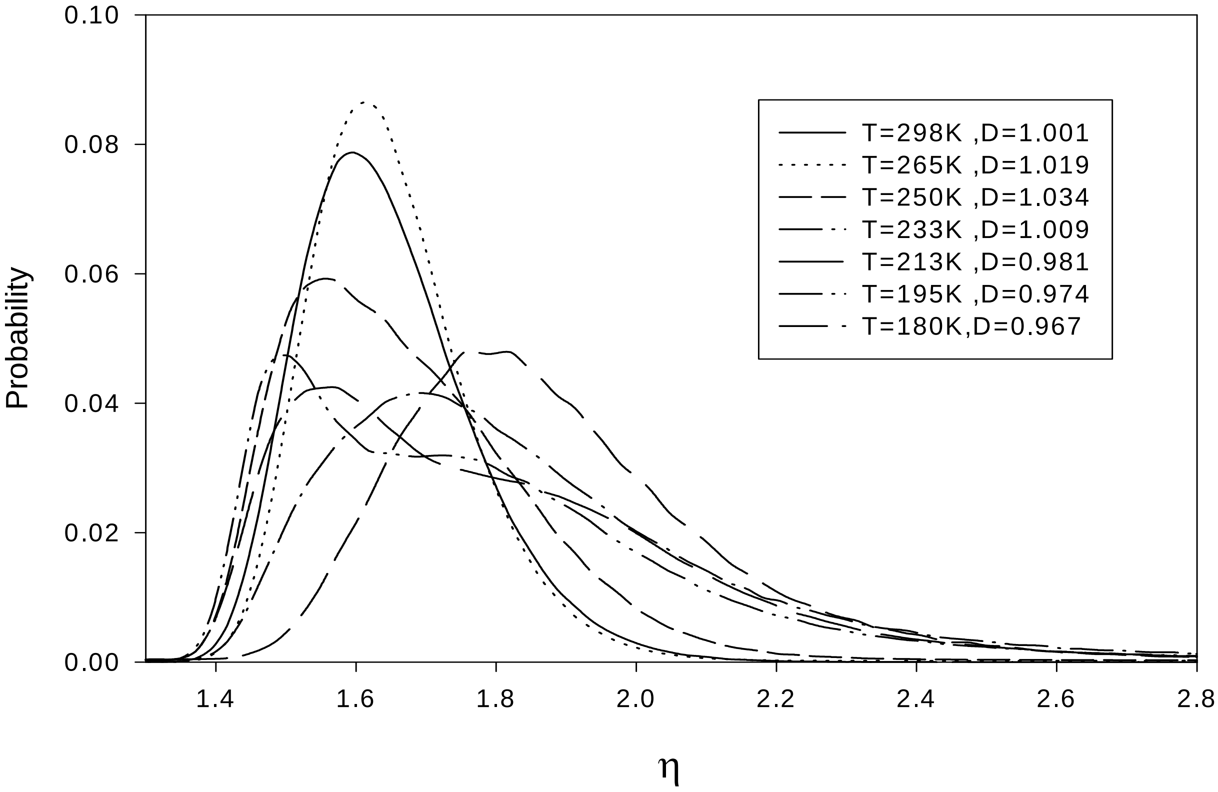

The asphericity distribution at different temperature shows two features. One is a two-component structure in liquid water; the broader the distribution the larger the volume fluctuation suggests the Cp maximum is located at 195K. Another feature is the structure lower than 180K is different from the one higher than 195K.

Radial Distribution Function

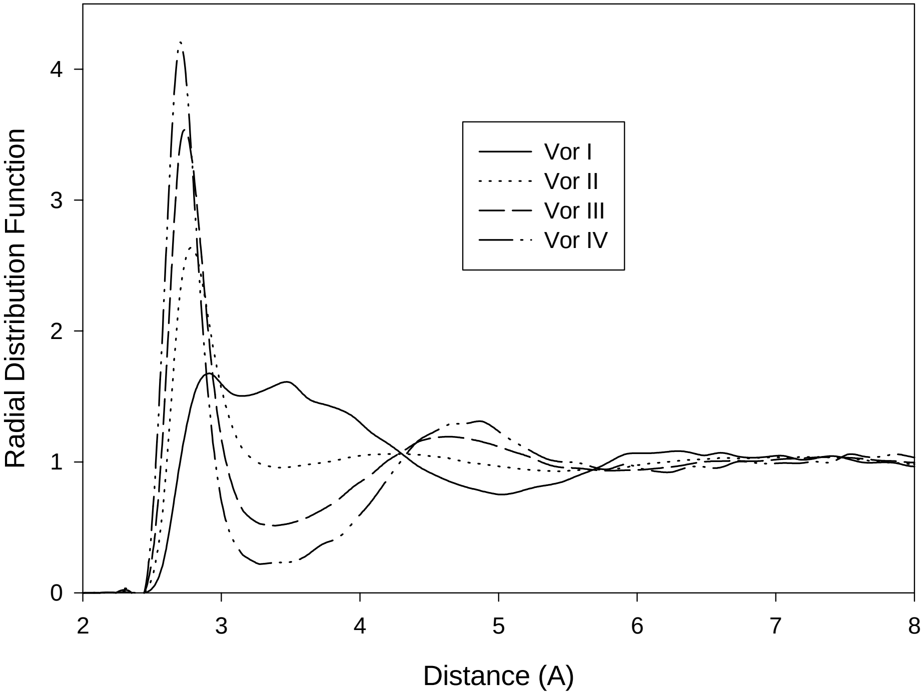

Oxygen-Oxygen pari correlation according to the asphericity(h) values of center reference molecule (TIP4P model) at 25°C, density=1.0 g/cm^3 in NVE ensemble. The isosbestic points located in 4.3, 5.7 and 6.9 Awere found in both SPC and TIP4P models, and can be taken as an indication of two coexisting structures in liquid water.

Spatial Distribution Function

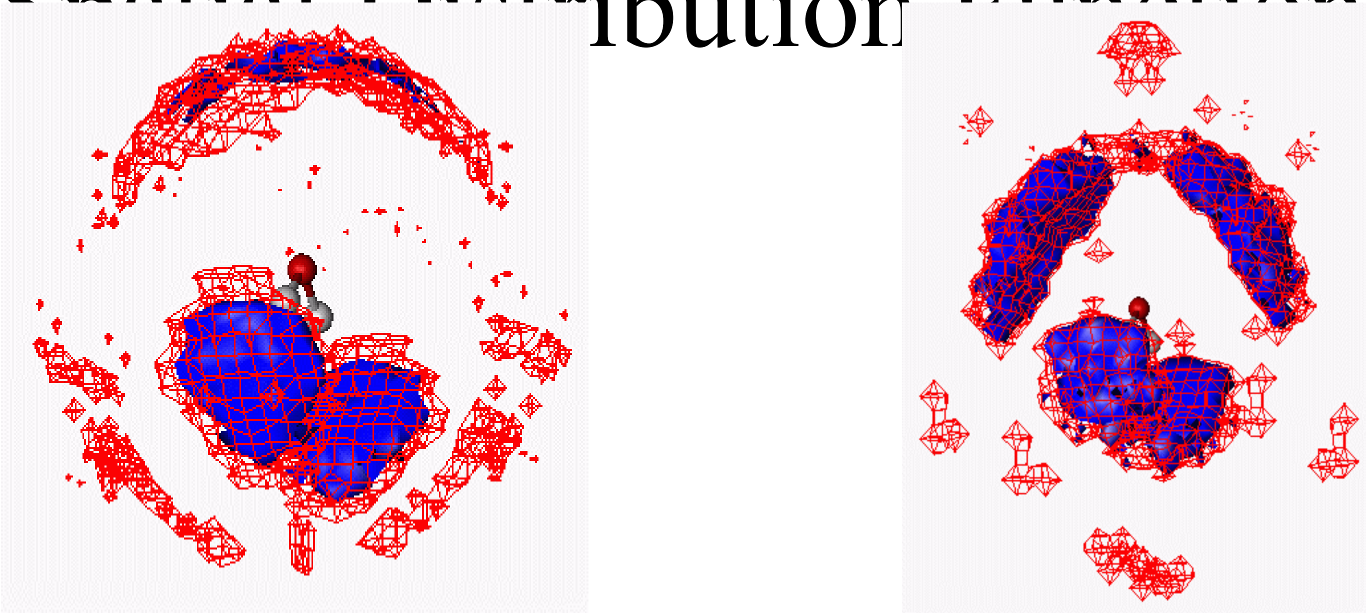

(a)Voronoi Section I

(b)Voronoi Section IV

The oxygen-oxygen spatial distributino function presented as a three-dimension map of thelocal oxygen density in liquid TIP4p water at 25°C. The iso-surface for $g_{OO}(r,W)=1.5$ is shownfor center reference molecule which is assigned as (a)Voronoi section I, a local randomness environment fulfilled with interstitial molecules. (b)Voronoi section IV, a ice-like local structure was develop for high asphericity value water. A broad bonding angle at the hydrogenacceptor site suggests a wide distribution in the hydrogen bond due to bending, as suggestedin the bend hydrogen bond model.

Dynamic Property

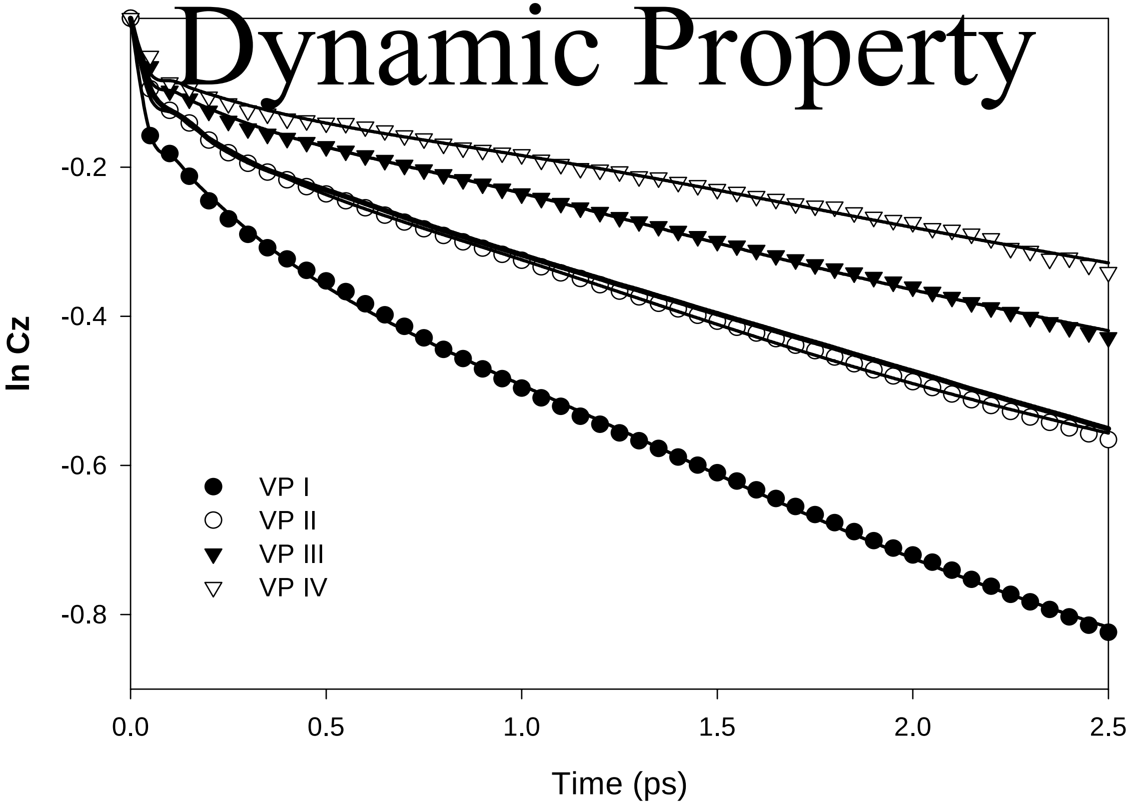

The scatter plots correspond to the second-order rotational autocorrelation function of the water dipole moment with different voronoi section center. The line plots are universal curve fitting with bi-exponential functions. The fast decay of the very short time would correspond to almost free inertial motion in water fluids and the two decay constants are t_R = 1.0 and 13 ps at 250K. The femtosecond mid-IR pump-probe spectroscopy of liquid water performed by Bakker shows the similar figures. This result suggests the slow and fast orientational dynamics are associated with locally cooperative rotation around the H-bond axis and with rototranslational coupling motion of the water molecule in a disordered cage.

Water supercooled in nanopore

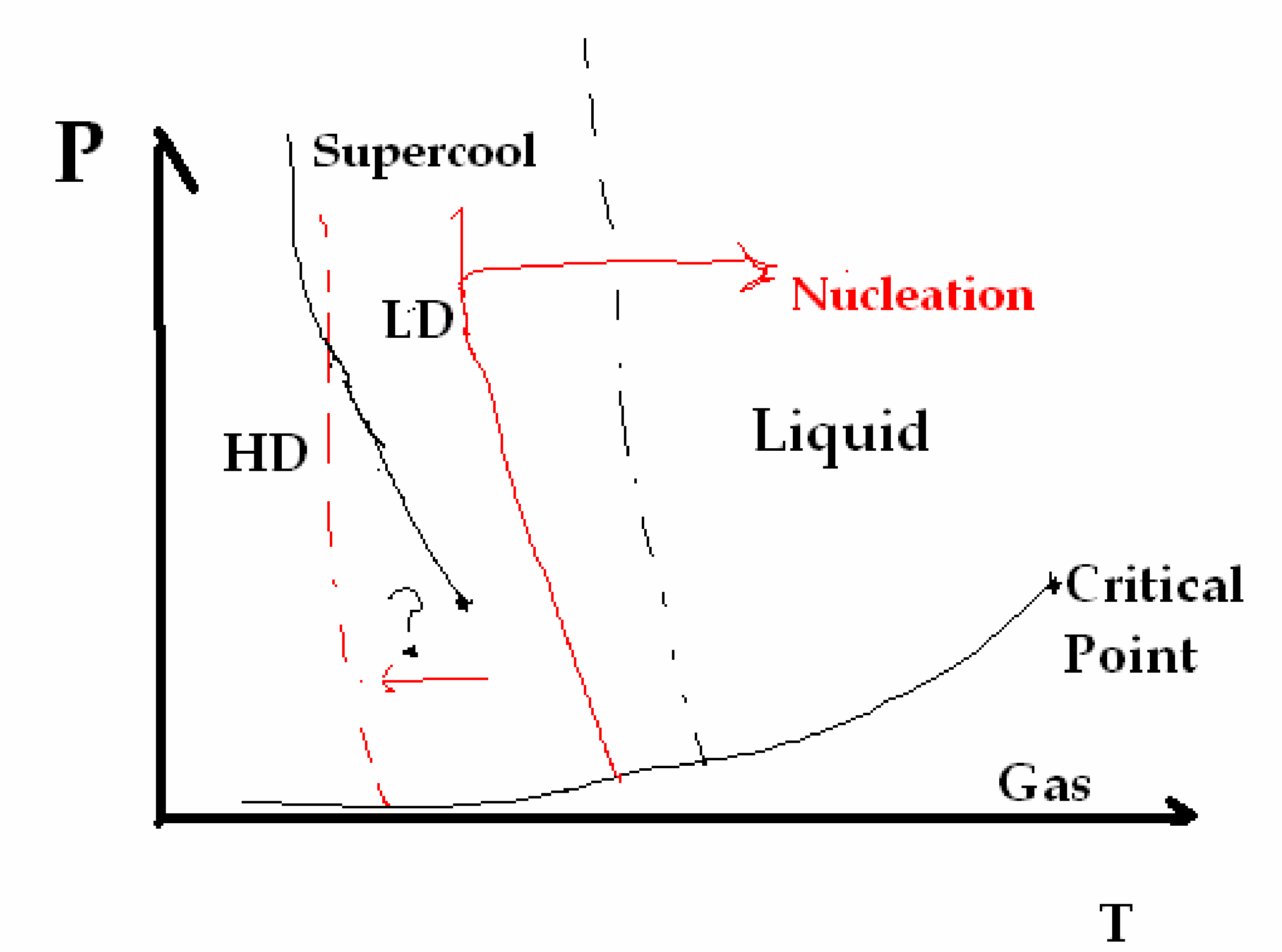

We avoid nucleation by confining water in nanopores.

Self-Assembling of Surfactant

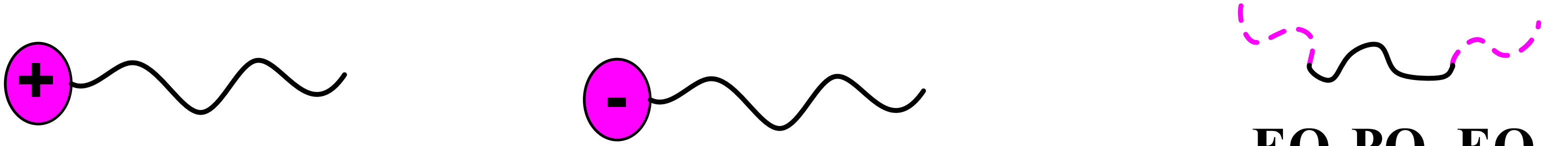

Cationic

Anionic

Neutral

EO PO EO

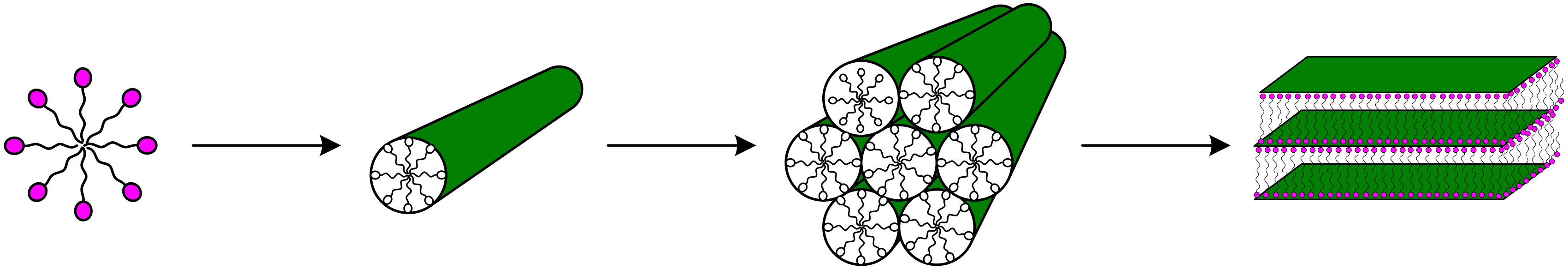

Sperical Micelles

Rod-like Micelles

Hexagonal Phase

Lamellar Phase

MCM-41-S Structure

MCM-41-S is well ordered with hexagonal symmetry.

Four MCM-41-S samples, fully hydrated:

Mac-110, with pore size <10 Å,

$\mathrm{gr}H_2O / \mathrm{gr}silica \approx 40\%$;

Mac-0912-6, with pore size 12 Å,

$\mathrm{gr}H_2O / \mathrm{gr}silica \approx 48\%$;

Mac-0124-4, with pore size 14 Å,

$\mathrm{gr}H_2O / \mathrm{gr}silica \approx 50\%$;

Mac-1219-7, with pore size 18 Å,

$\mathrm{gr}H_2O / \mathrm{gr}silica \approx 55\%$.

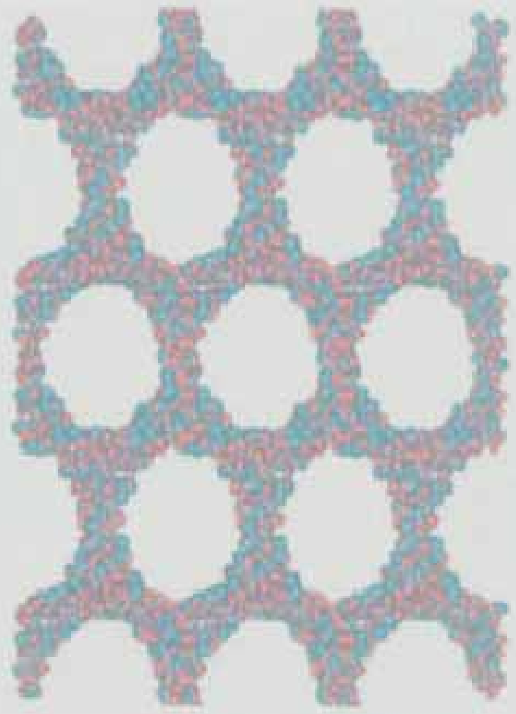

MCM-41 structure

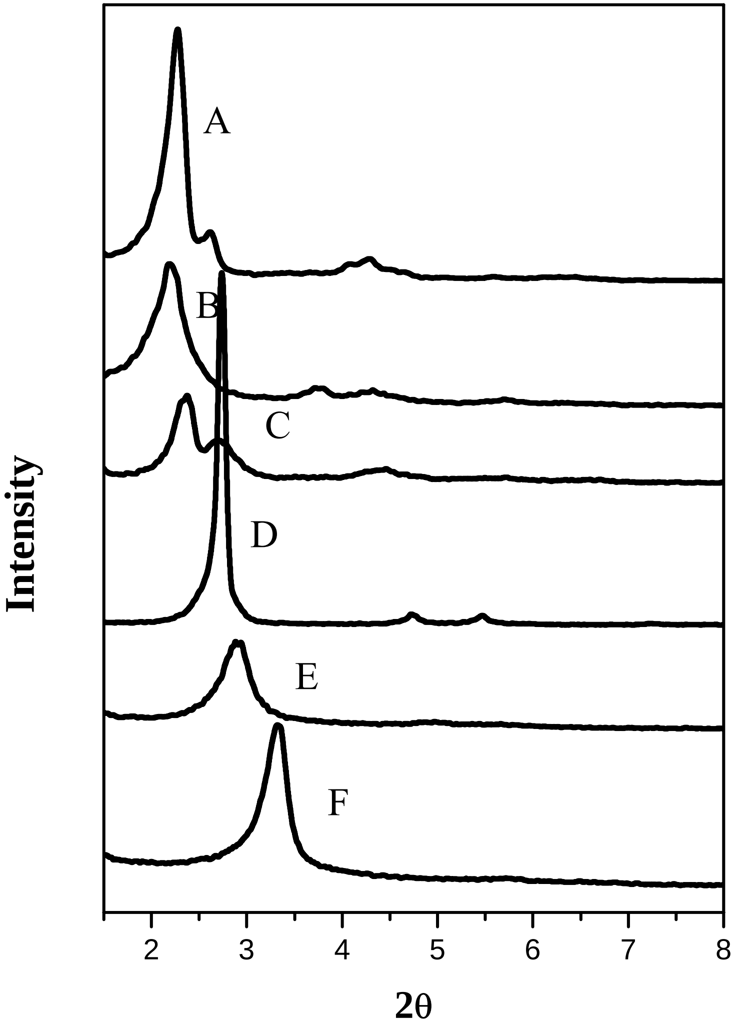

Intensity
A
B
C
D
E
F
2
3
4
5
6
7
8
2θ

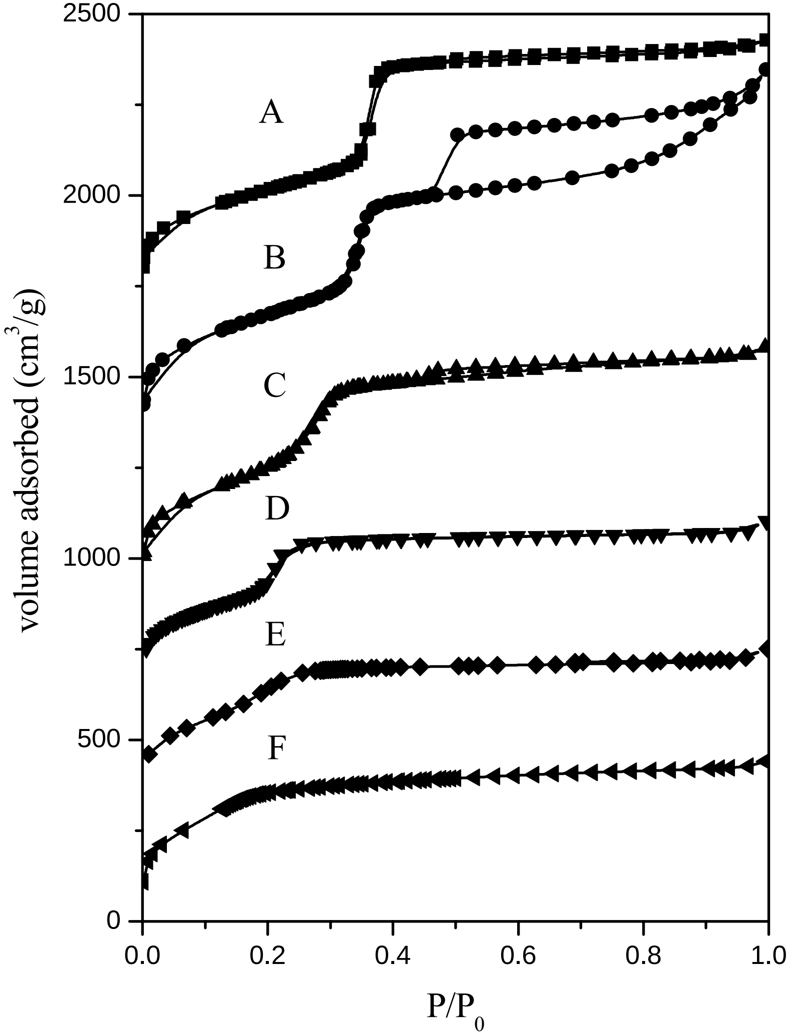

volume adsorbed (cm^3/g)
2500
2000
1500
1000
500
0
A
B
C
D
E
F
0.0
0.2
0.4
0.6
0.8
1.0
P/P$_0$

Differential Scanning Calorimetry

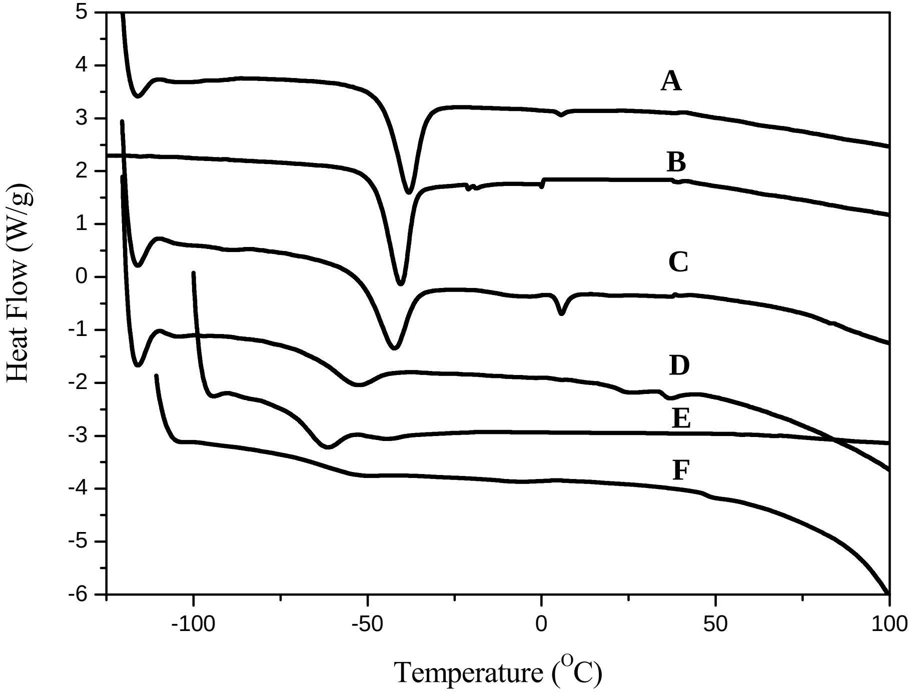

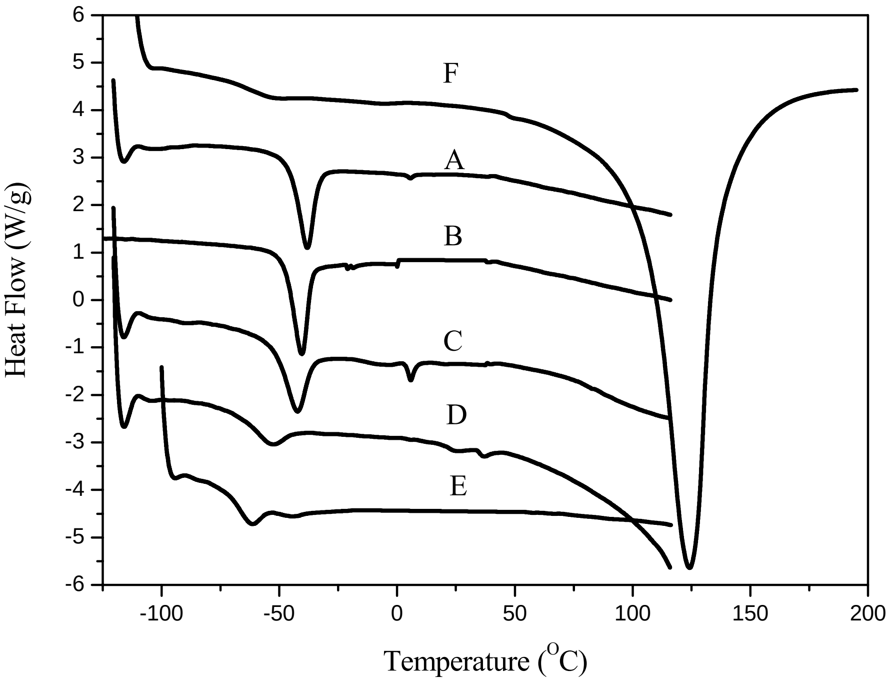

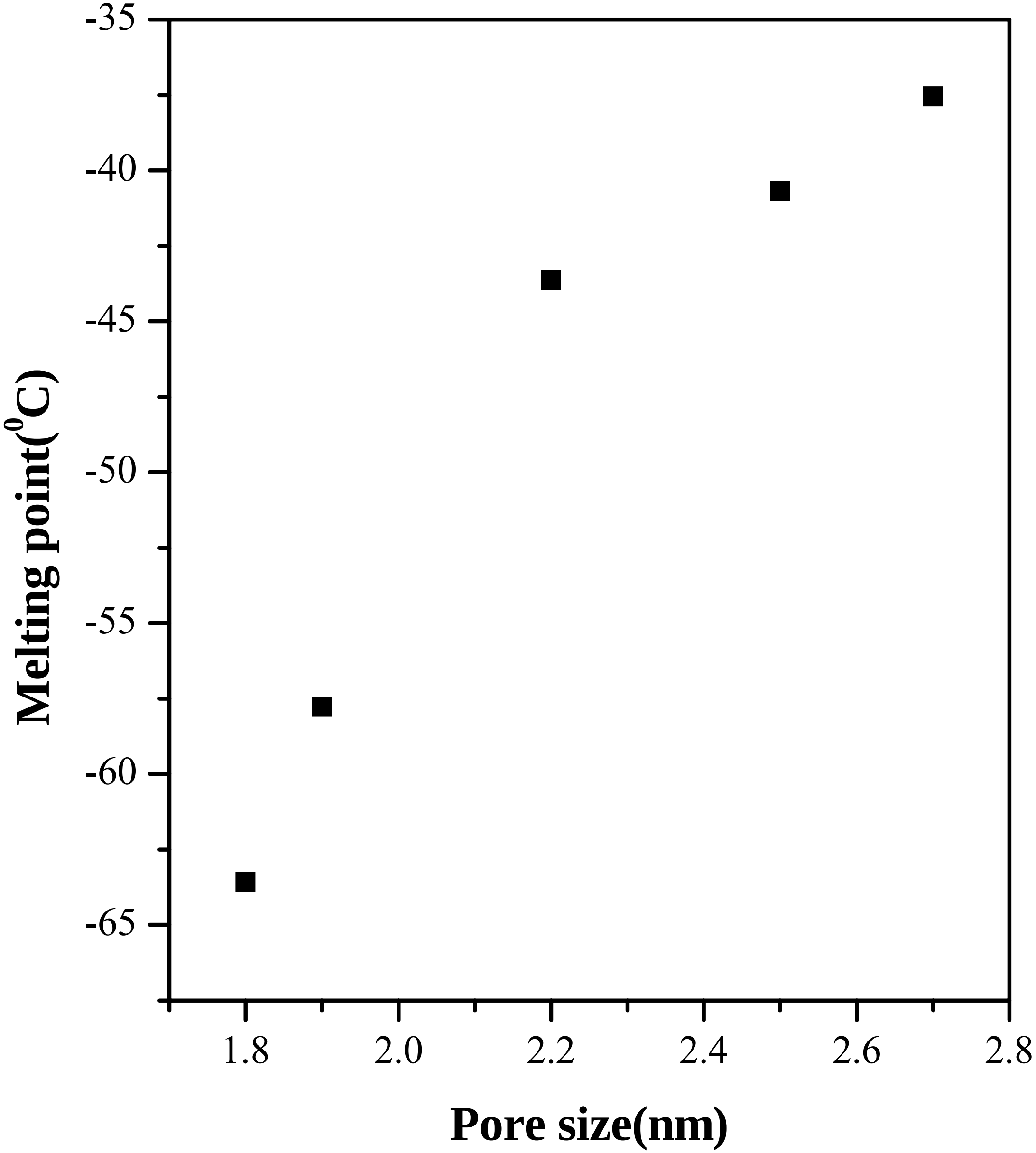

-35
-40
-45
-50
-55
-60
-65
Melting point(^{0}C)
1.8
2.0
2.2
2.4
2.6
2.8
Pore size(nm)

QENS Experiments

$$\frac{d^2\sigma_H}{d\Omega d\omega} = 2N\frac{\sigma_H}{4\pi}\frac{k_f}{k_i}S_H(Q,\omega)$$

Measure the number of scattered neutrons
as a function of Q and ω

$$S_H(Q,\omega) = \frac{1}{\pi}\int_0^\infty dt\,\cos\omega t\, F_H(Q,t)$$

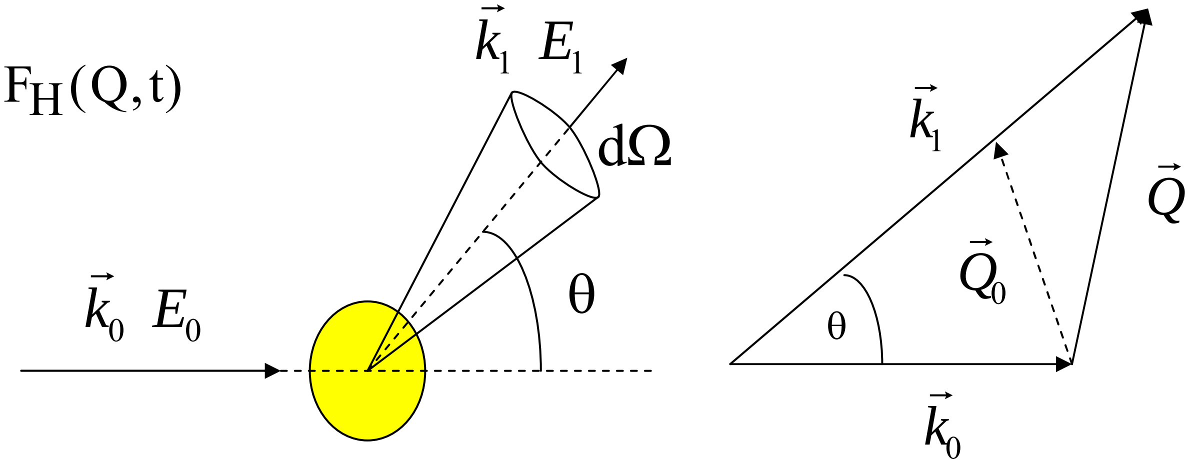

NIST Center for Neutron Research:

Disk Chopper (DCS) and Backscattering (HFBS) spectrometers with resolutions 30 μeV and 1 μeV respectively, have Q ranges: 0.2 Å^{-1} - 2.0 Å^{-1}, which is broad enough to simultaneously measure both translational and rotational dynamics of the water molecules.

The data can be analyzed according to the equation

$$S(Q,\omega) = pR(Q_0,\omega) + (1-p)FT\left\{F_H(Q,t)R(Q_0,t)\right\}$$

The decoupling approximation has been generally assumed in the data analysis and the ISF of the hydrogen atom can be written as:

$$F_H(Q,t) = F_T(Q,t) \cdot F_R(Q,t)$$

$$F_R(Q,t) = \sum_{l=0}^{\infty}(2l+1)j_l^2(Qb)C_l(t)$$

$$F_T(Q,t) = F_T^s(Q,t)\exp[-(t/\tau_T)^{\beta}]$$

$$\tau_T = \tau_0(aQ)^{-\gamma}$$

$$C_1(t) = C_1^s(t)\exp\,[-(t/\tau_R)^{\beta}]$$

β: The stretch exponent.

$\beta\gamma$: The actual exponent of the Q dependence of the ISF.

$\langle\tau_0\rangle = (\tau_0/\beta)\Gamma(1/\beta)$: Average translational relaxation time.

$\langle\tau_R\rangle = (\tau_R/\beta)\Gamma(1/\beta)$: Average rotational relaxation time.

A. Faraone, L. Liu, et al**, “**Translational and Rotational Dynamics of Water in Mesoporous Silica Materials: MCM-41-S and MCM-48-S**”**, *J. Chem. Phys.* **119**, 3693 (2003)

Relaxing-Cage Model

On lowering the temperature below the freezing point, there is a tendency to form around a given water molecule a hydrogen-bonded, tetrahedrally coordinated first neighbor shell (cage). At short times, less than 0.05 ps, the water molecule performs harmonic vibrations and librations inside the cage. At long times, longer than 1.0 ps, the cage eventually relaxes and the trapped particle can migrate through the rearrangement of a large number of particles surrounding it. Thus, there is a strong coupling between the single particle motion and the density fluctuations of the fluid.

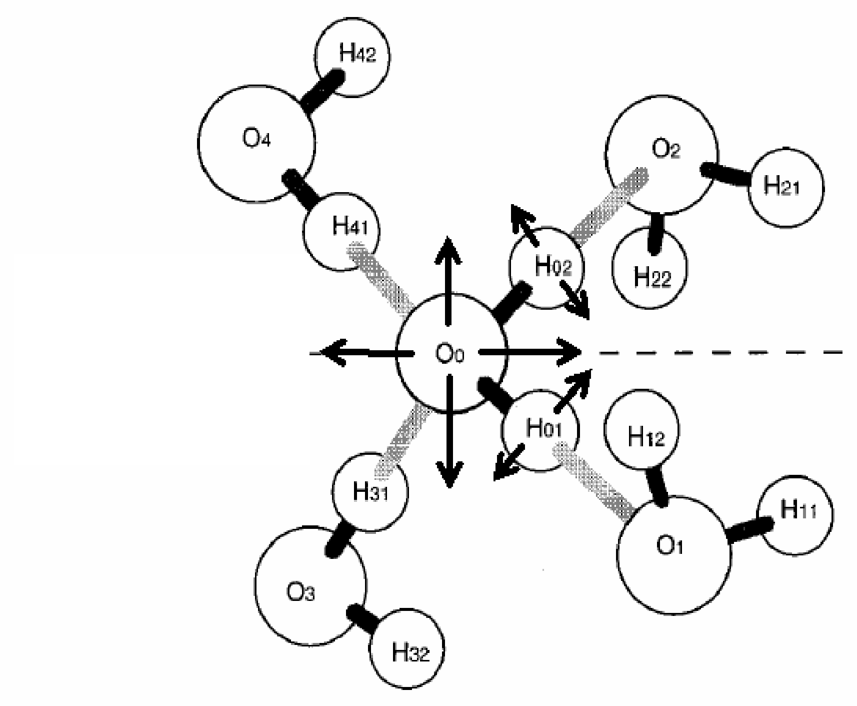

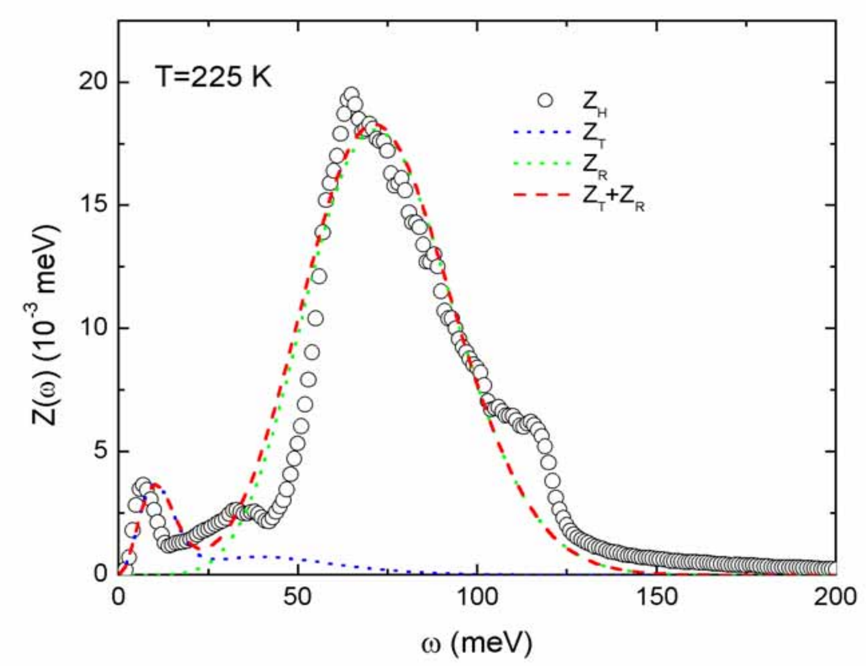

Model for the Translational Dynamics

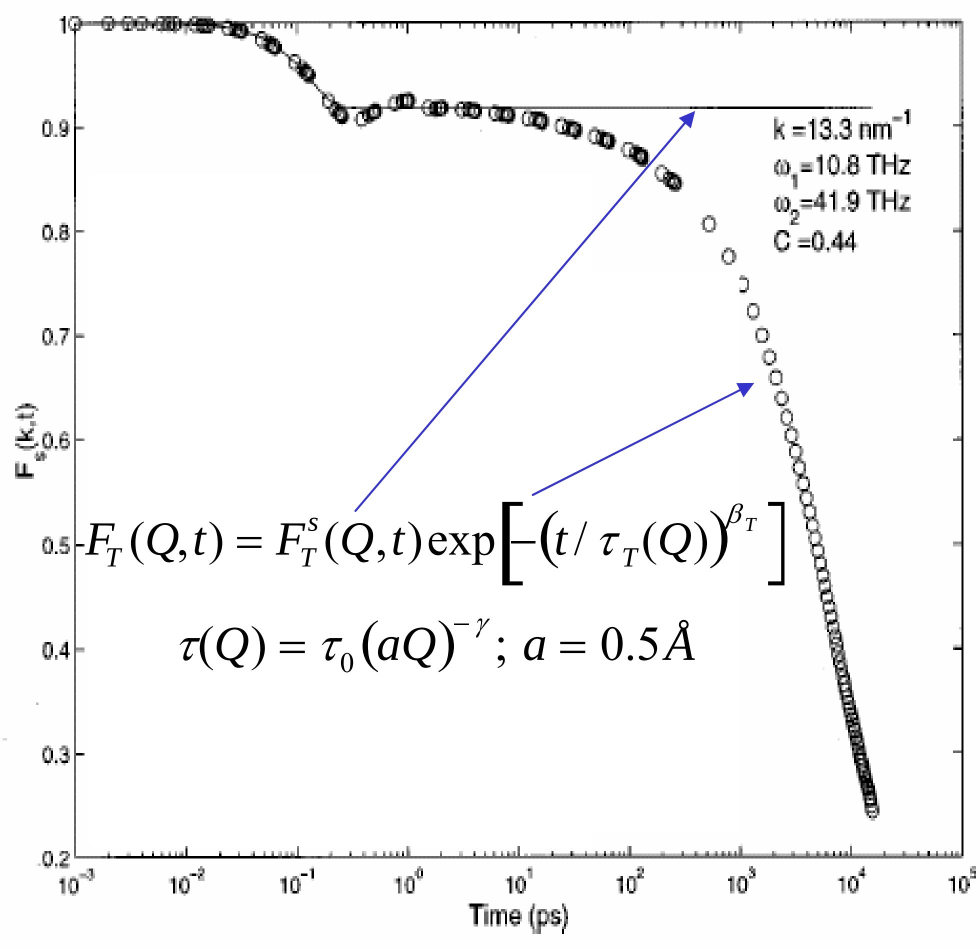

$$F_T(Q,t) = F_T^s(Q,t)\exp\left[-\left(t/\tau_T(Q)\right)^{\beta_T}\right]$$

$$\tau(Q) = \tau_0 (aQ)^{-\gamma};\ a = 0.5\mathring{A}$$

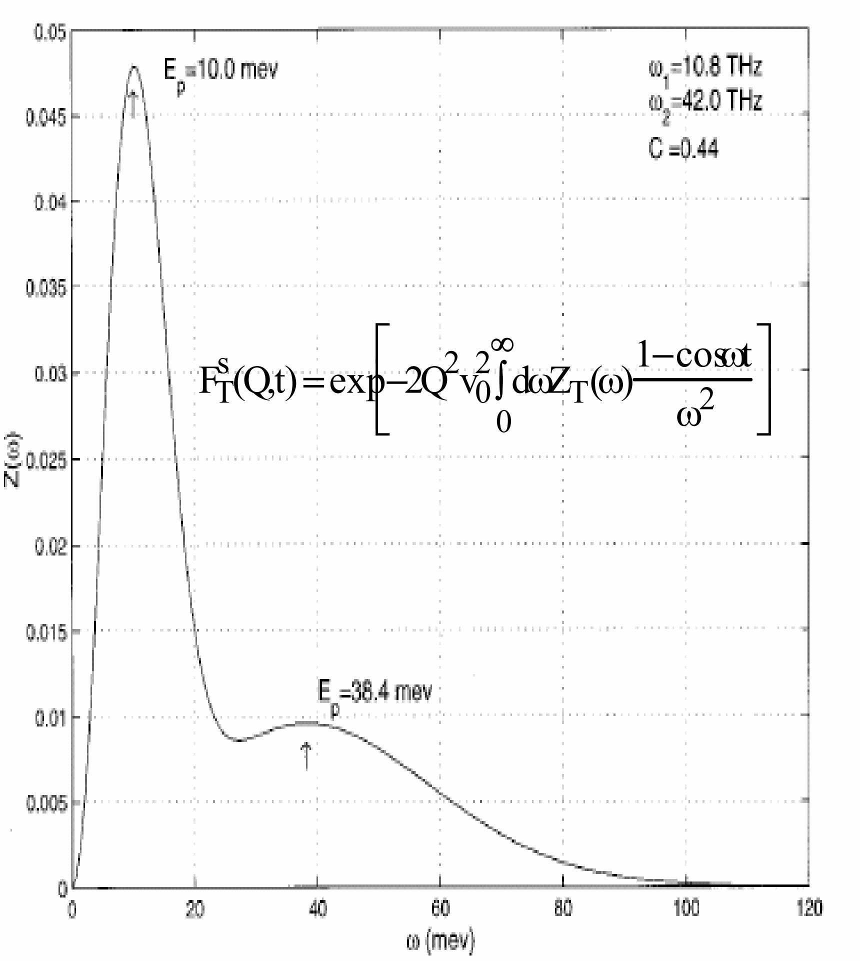

$$F_T^s(Q,t) = \exp\left[-2Q^2 v_0^2 \int_0^\infty d\omega Z_T(\omega)\frac{1-\cos\omega t}{\omega^2}\right]$$

S. H. Chen, C. Liao, F. Sciortino, P. Gallo, P. Tartaglia, “Model for single-particle dynamics in supercooled water”, *Phys. Rev. E* **59**, 6708 (1999)

S.L. Chang, Ten-ming Wu, and Chung-Yuan Mou, *J Chem. Phys.*, 121, 3605(2004)

"Instaneous Normal Mode analysis of Orientational Motion in Liquid Water"

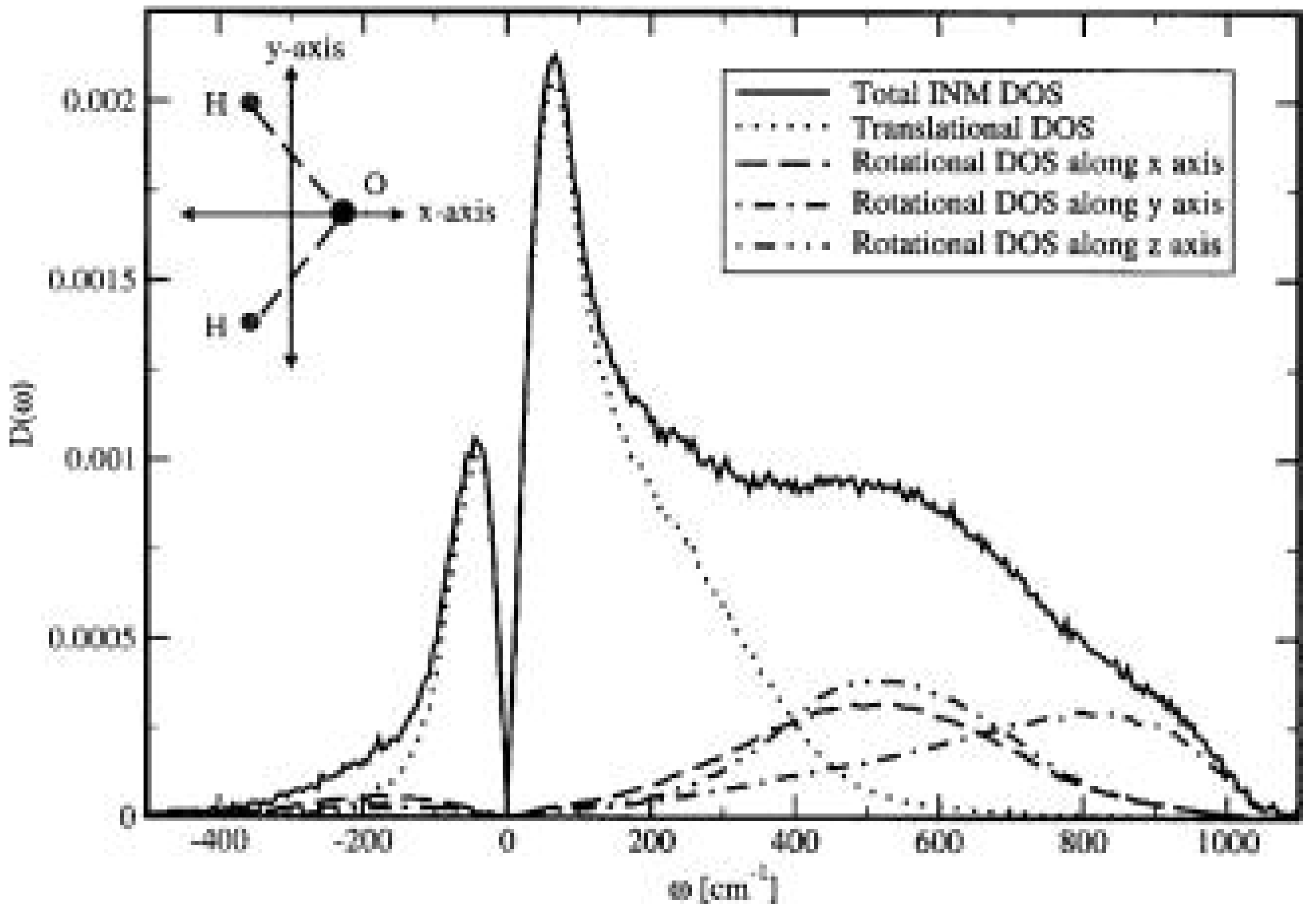

The Model for Rotational Dynamics

At supercooled temperatures, water molecules are constrained in the cages formed by their neighbors through H-bonds.

- *At short times, they perform harmonic librational motions.*
- *At longer times, the cages relax according to a stretch exponential decay.*

$$F_R(Q,t) = \sum_{l=0}^{\infty}(2l+1)j_l^2(Qb)C_l(t)$$

$$C_1^s(t) = \exp\left[-\frac{4}{3}\left\langle\omega^2\right\rangle\int_0^{\infty}d\omega\, Z_R(\omega)\frac{1-\cos\omega t}{\omega^2}\right]$$

$$C_1(t) = C_1^s(t)\exp\left[-\left(t/\tau_R\right)^{\beta}\right]$$

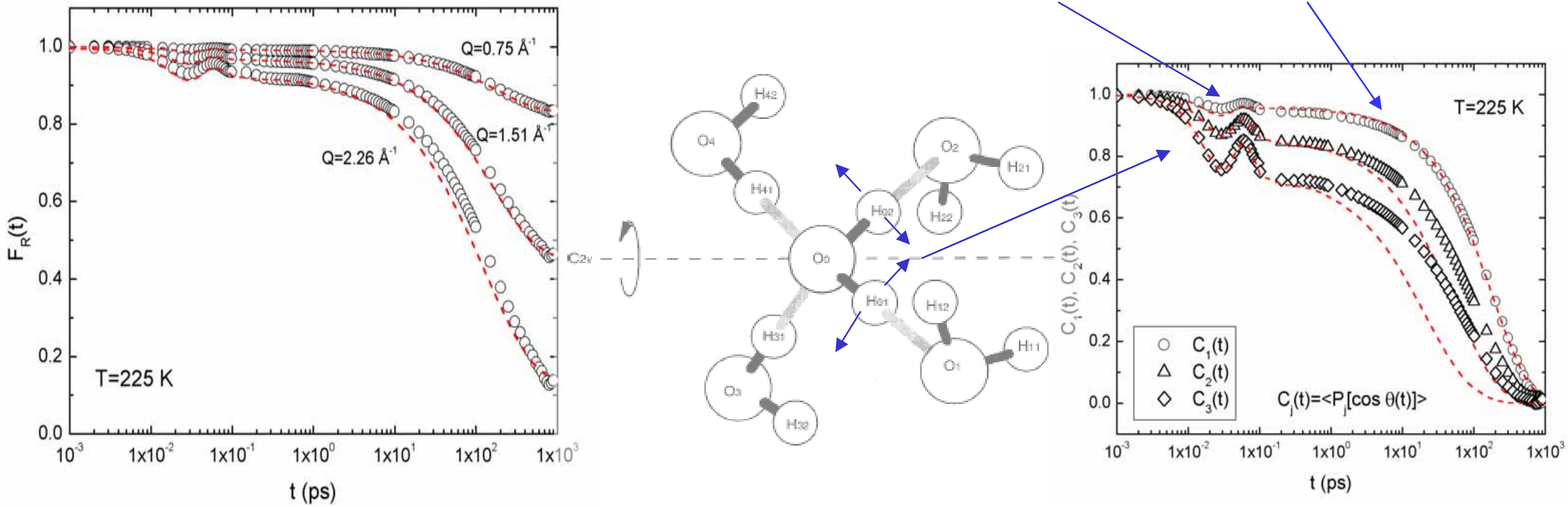

L. Liu, A. Faraone, S. H. Chen, “Model for the rotational contribution to quasielastic neutron scattering spectra from supercooled Water”, *Phys. Rev. E* **65**, 041506 (2002)

Fitting Results

The figure shows the results of the model fit including the first three terms of Sears expansion:

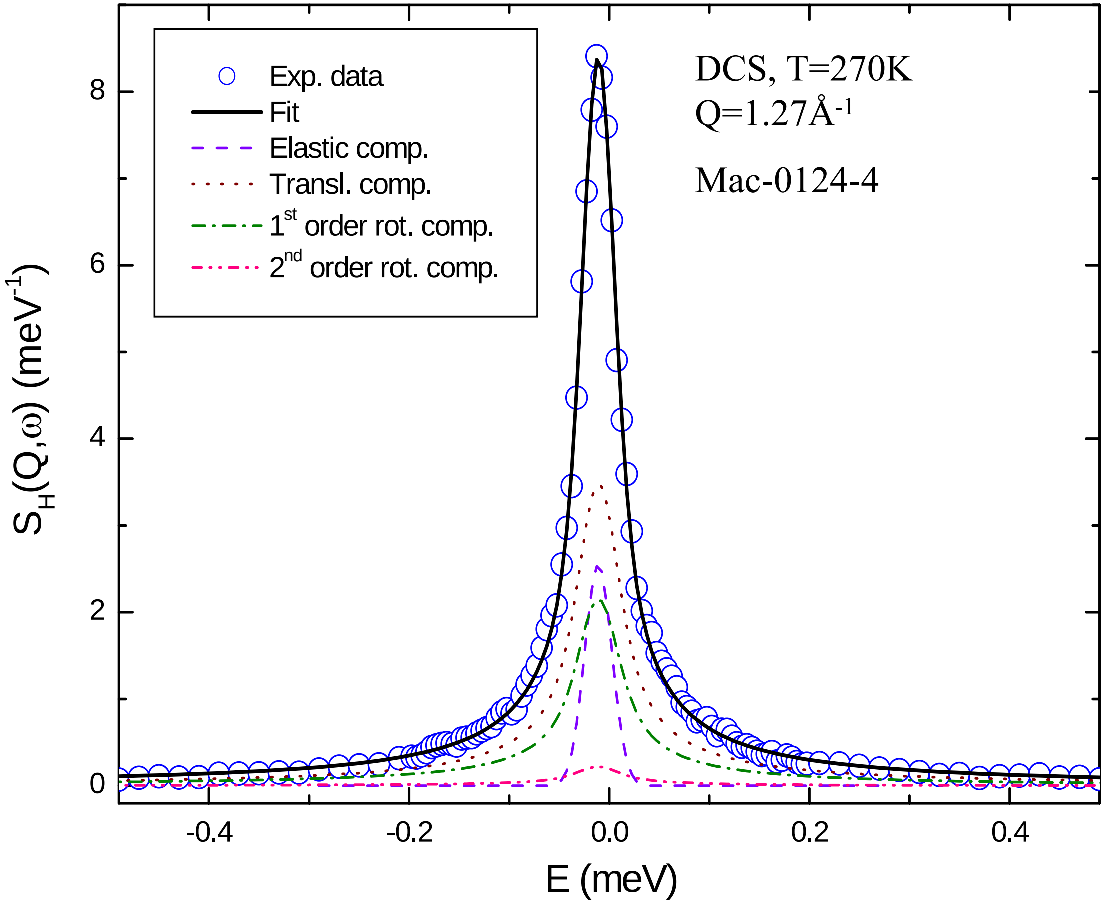

Translation comp:

$$FT\{F_T \cdot j_0^2(Qb)\}$$

1st order rotation comp:

$$FT\{F_T \cdot 3j_1^2(Qb) \cdot C_1(t)\}$$

2nd order rotation comp:

$$FT\{F_T \cdot 5\,j_2^2(Qb) \cdot C_2(t)\}$$

High Resolution QENS Spectra and Their Analysis

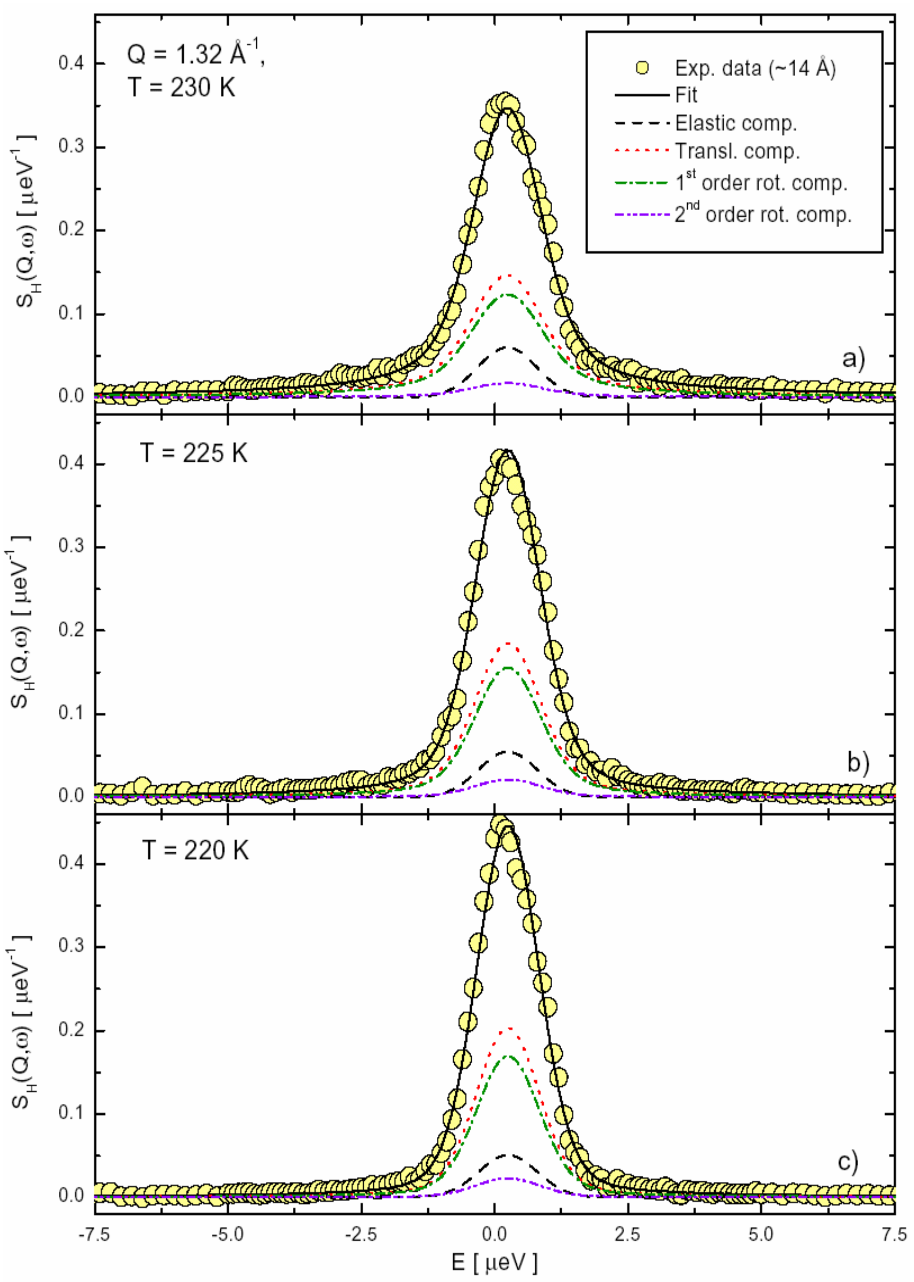

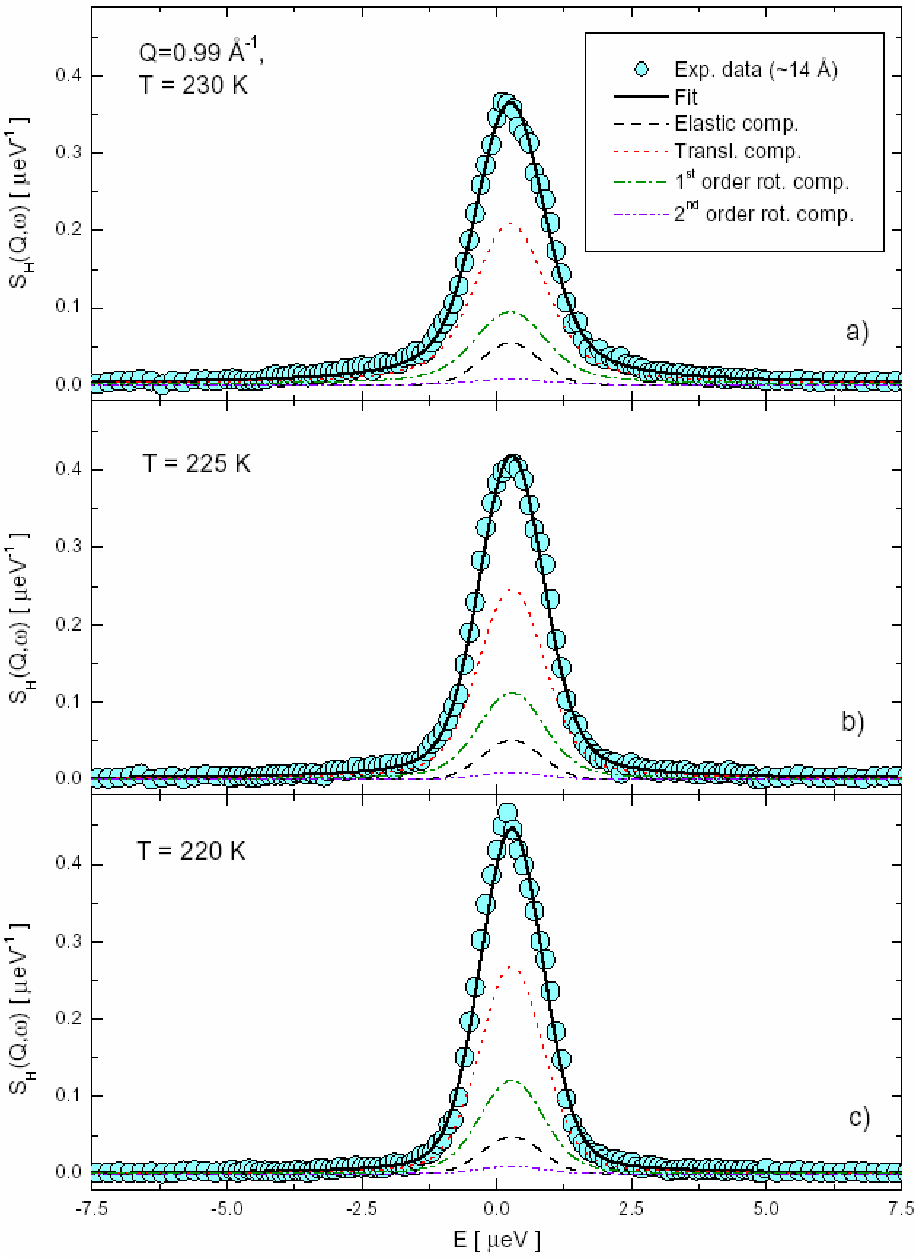

Temp. Dependence of Ave. Trans. Relax. Times

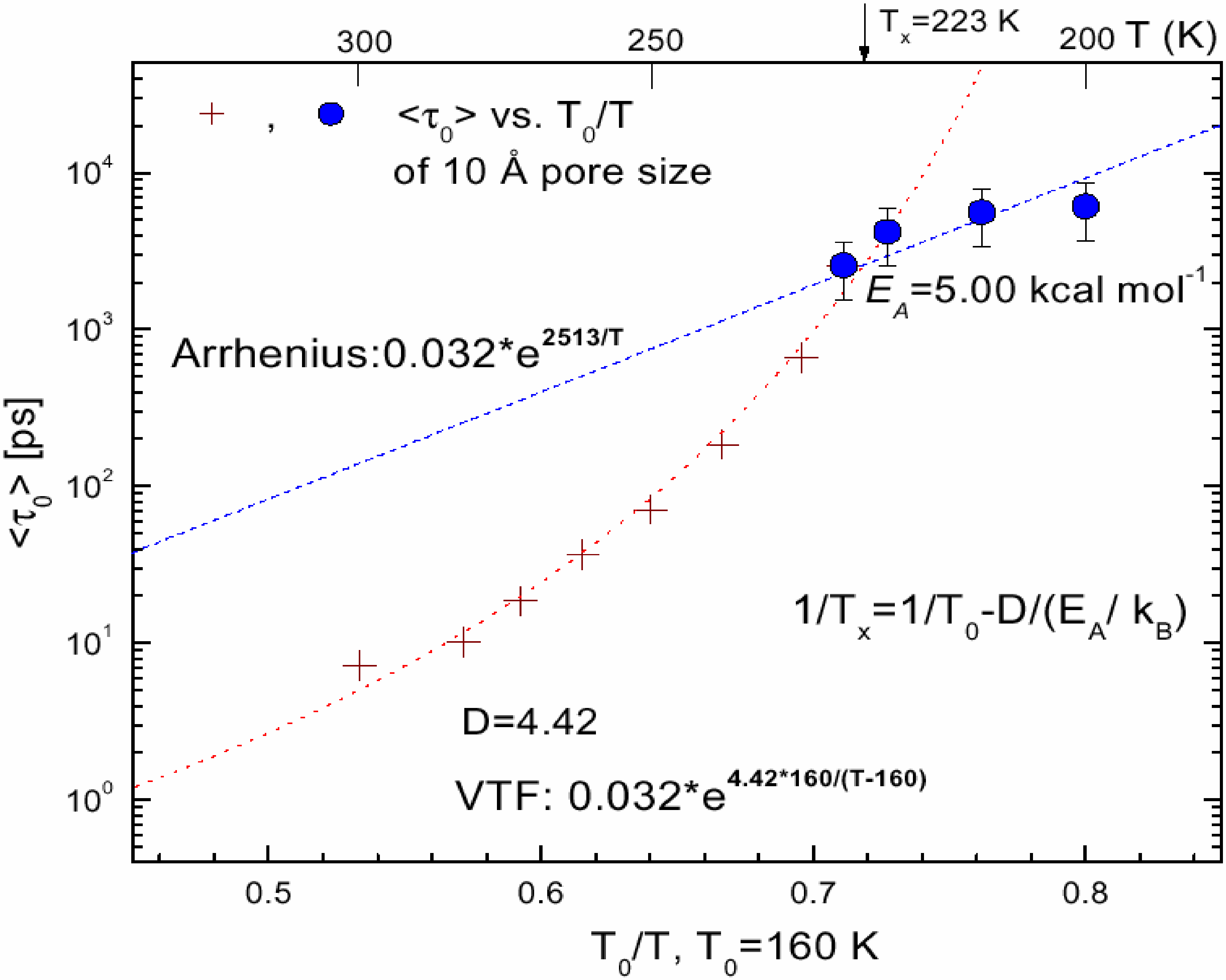

Temp. Dependence of Ave. Trans. Relax. Times

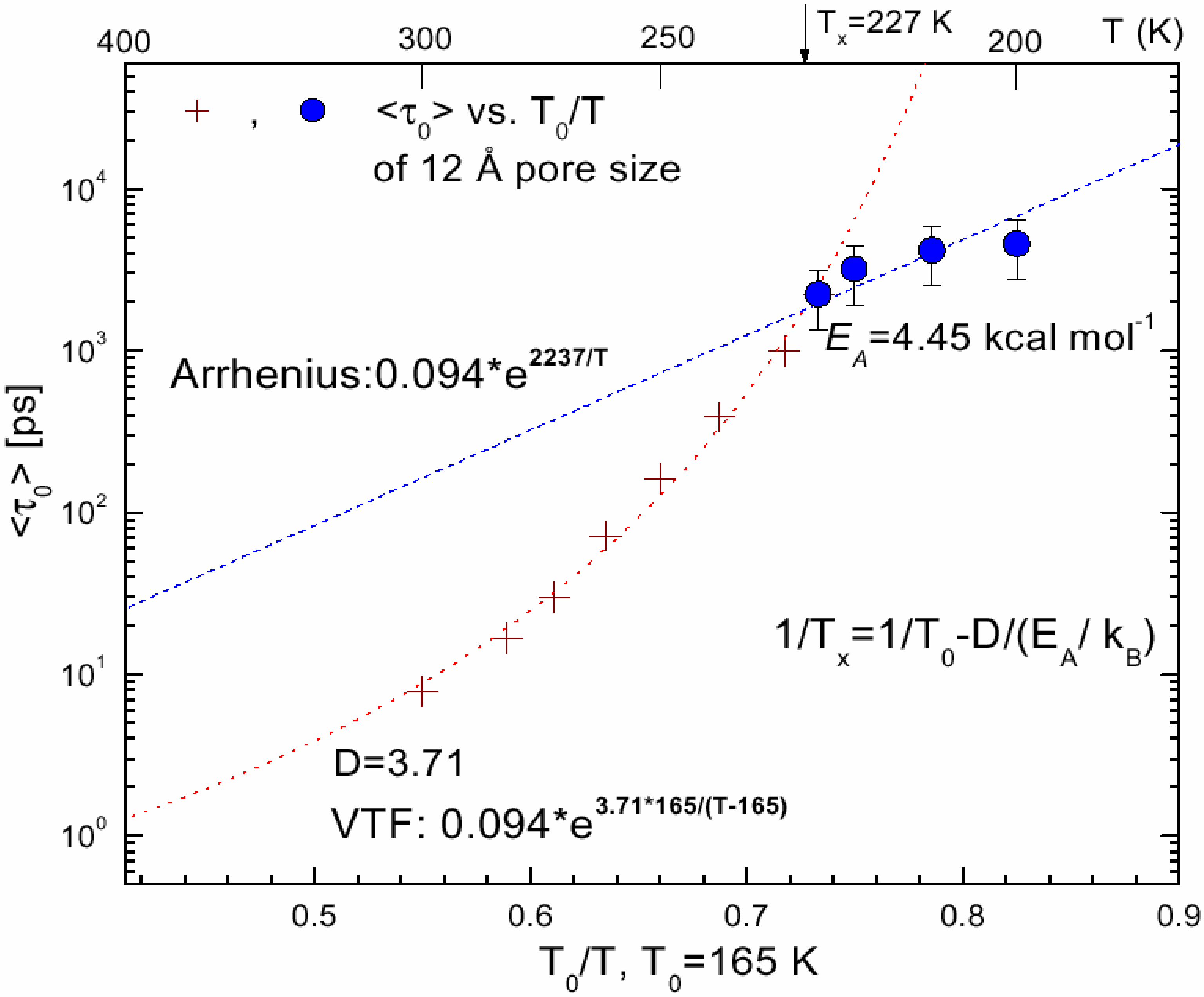

Temp. Dependence of Ave. Trans. Relax. Times

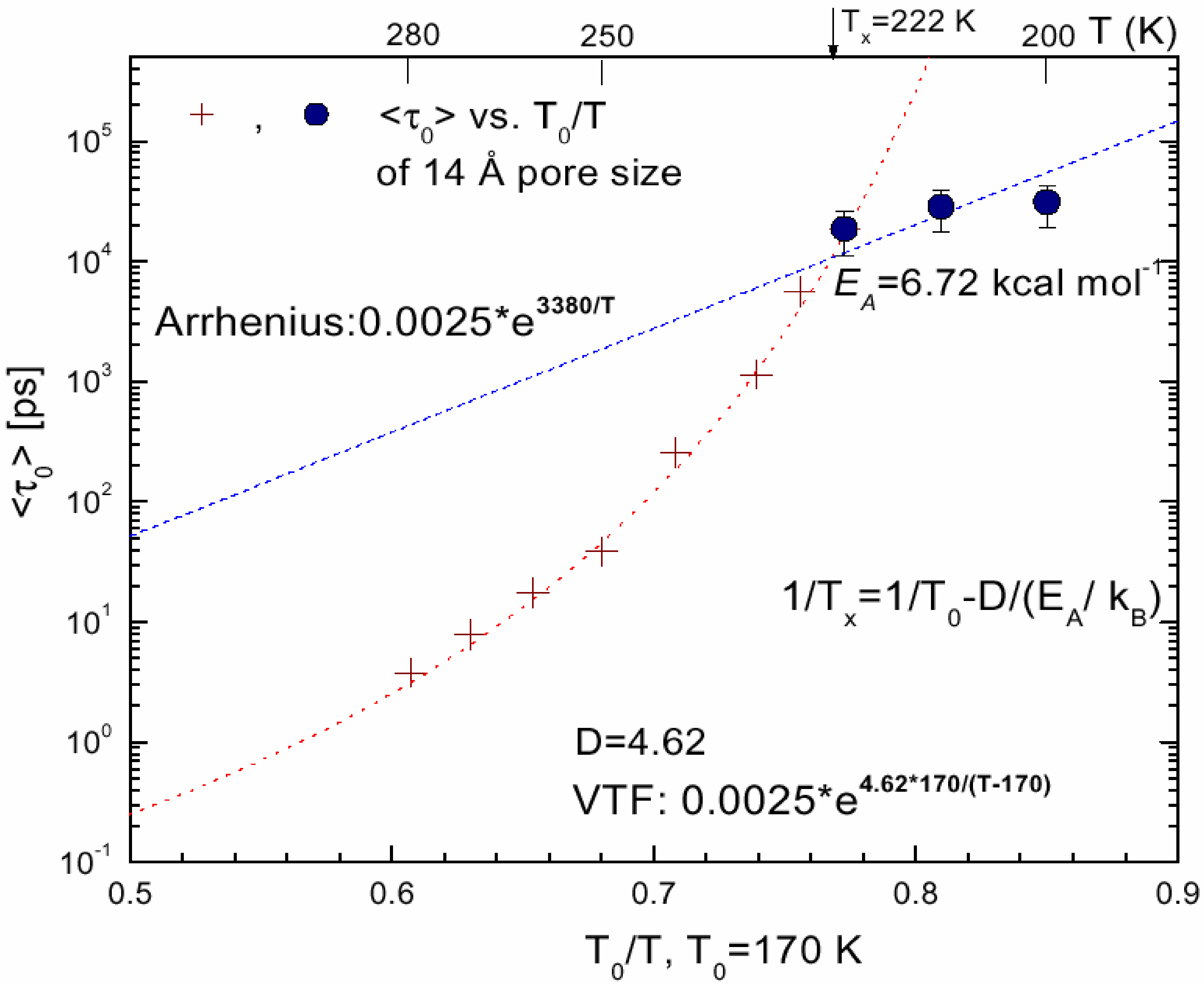

Temp. Dependence of Ave. Trans. Relax. Times

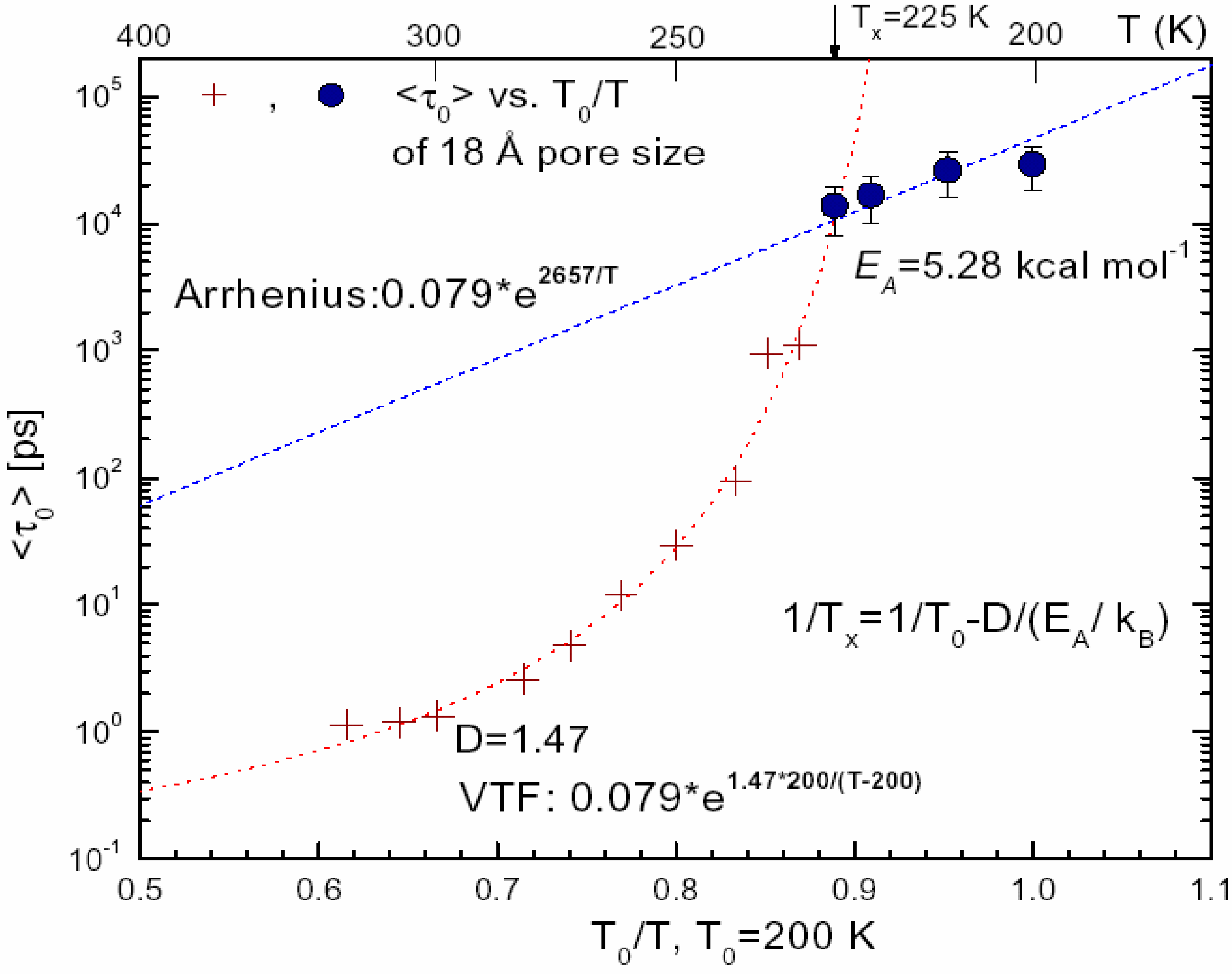

Q-Dep. of the Translational ISF

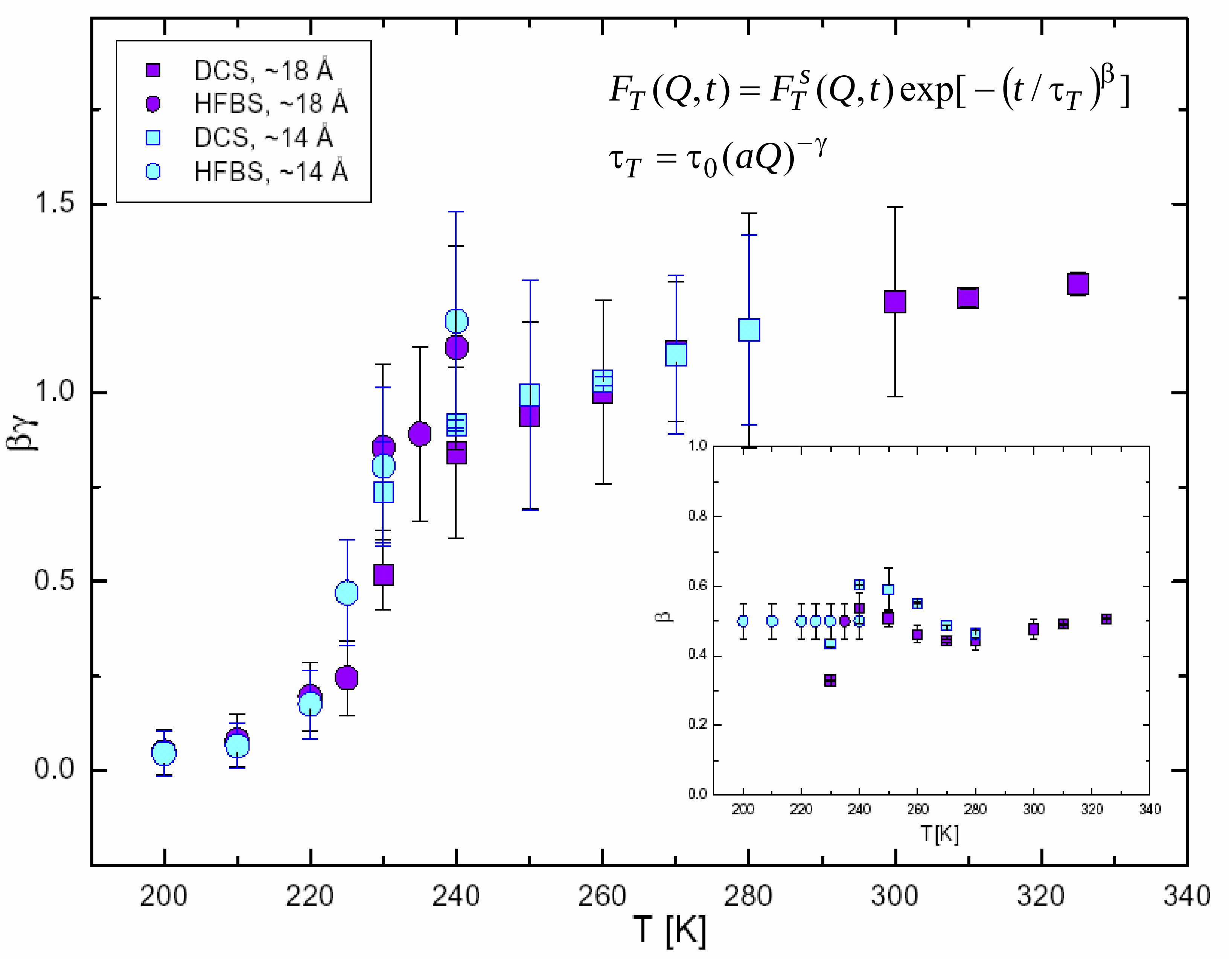

$$F_T(Q,t) = F_T^s(Q,t)\exp[-(t/\tau_T)^{\beta}]$$

$$\tau_T = \tau_0(aQ)^{-\gamma}$$

Ave. Translational Relaxation Time measured by QENS

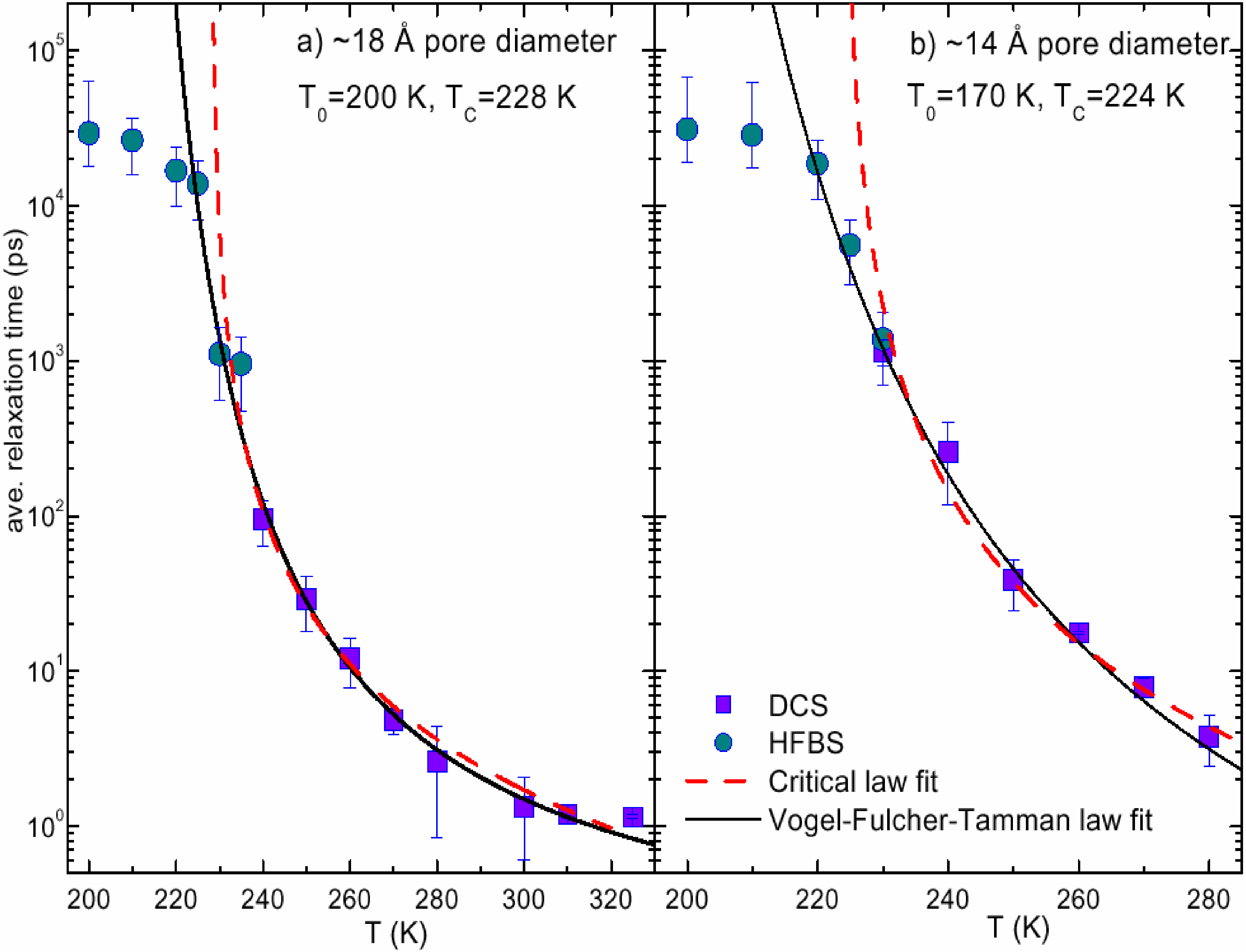

致謝：

臺灣大學

- 葉玉玲
- 閻君婉
- 施貝淳

NRC, Canada
Dr. John Tse

經費

- 國科會

MIT:

- **Prof. S.H. Chen**
- **Dr. A. Faraone**
- **Ms. L. Li**

交通大學

- 吳天鳴教授
- **Dr. S.L. Chang**